INTERNATIONAL JOURNAL OF ROBUST AND NONLINEAR CONTROL
Int. J. Robust. Nonlinear Control 2013; **00**:1–25
Published online in Wiley InterScience (www.interscience.wiley.com). DOI: 10.1002/rnc

A Globally Asymptotically Stabilizing Trajectory Tracking Controller for Fully Actuated Rigid Bodies using Landmark-based Information

Pedro Casau[1], Ricardo G. Sanfelice[2], Rita Cunha[1], Carlos Silvestre[1,3]

[1] *Department of Electrical Engineering and Computer Science, and Laboratory for Robotics and Systems in Engineering and Science (LARSyS), Instituto Superior Técnico, Universidade Técnica de Lisboa, 1049-001 Lisboa, Portugal*

[2] *Department of Computer Engineering, University of California, Santa Cruz, CA 95064, USA.*

[3] *Department of Electrical and Computer Engineering, Faculty of Science and Technology of the University of Macau*

SUMMARY

In this paper, we address the problem of designing a control law based on sensor measurements that provides global asymptotic stabilization to a reference trajectory defined on the $SE(3) \times \mathbb{R}^6$. The proposed control law is a function of the angular velocity, of vector measurements characterizing the position of some given landmarks and of their rate of change. We provide sufficient conditions for the existence of synergistic potential functions on $SO(3)$ which are pivotal in the generation of a suitable hybrid control law. We also provide sufficient conditions on the geometry of the landmarks to solve the given problem. Finally, the proposed solution is simulated and compared with a continuous feedback control law. Copyright © 2013 John Wiley & Sons, Ltd.

Received ...

1. INTRODUCTION

The attitude control problem has been a long-standing challenge within the control engineering community and it has generated a large number of contributions [1, 2, 3]. This problem consists of stabilizing the attitude of a rigid body to a desired point regardless of the initial condition. There are several reasons for the general interest in solving this problem: (1) the attitude is described by an element of the special orthogonal group of order three, denoted by $SO(3)$, which is a compact manifold without boundary, thus topological obstructions preclude global stabilization of a set-point by means of continuous feedback [4]. In particular, given a Morse function $f : M \to \mathbb{R}$ defined on a compact manifold M, every flow determined by the gradient vector field converges to the critical points of f (cf. [5, Lemma 2.23]). Since every Morse function in $SO(3)$ has at least 4 critical points (cf. [2, p.148]), global stabilization of a single set-point is not possible; (2) there exist several

[†]The work of Pedro Casau was supported with grant SFRH/BD/70656/2010 from Fundação para a Ciência e a Tecnologia. Research by Carlos Silvestre has been supported by Project MYRG118(Y1-L3)-FST12-SSW of the University of Macau and ONRg N62909-14-1-V234 grant. Research by Ricardo G. Sanfelice has been partially supported by the National Science Foundation under CAREER Grant no. ECS-1150306 and by the Air Force Office of Scientific Research under Grant no. FA9550-12-1-0366. The work of Rita Cunha was supported by the FCT Investigator Programme (IF/00921/2013). This work was partially supported by the Fundação para a Ciência e a Tecnologia (FCT) under the project PEst-OE/EEI/LA0009/2013

parametrizations of $SO(3)$, each of which has its own advantages/disadvantages, depending on the application [6]; (3) there exists a myriad of applications where attitude control is key, including the control of spacecraft [7, 8, 9, 10], aerial vehicles [11] and underwater vehicles [12].

Possible parametrizations of $SO(3)$ include Euler angles, Euler parameters, quaternions, among many others (see [13]), all of which exhibit either singularities or ambiguities at some point (cf. [14], [15]). Nevertheless, the quaternion parametrization of $SO(3)$ has been used in several applications during the last decades [16, 12, 17]. In particular, the work reported in [12], provides an extensive list of different quaternion-based feedback laws as well as the advantages and drawbacks of each individual choice. Despite their wide acceptance and although the quaternions provide a global parametrization of $SO(3)$, they consist of a many-to-one map which is bound to cause some problems namely: inconsistent path-lifting [18] and/or it may lead to the so called "unwinding phenomenon" [4]. On the other hand, the rotation matrix description of attitude is global and unique [15], thus it can be computed out of vector measurements without ambiguity [19, 20]. The relationship between vector measurements and the rotation matrix is of particular significance for the work developed in this paper.

A solution to global stabilization on $SO(3)$ was firstly proposed in [12] by means of discontinuous quaternion feedback and then adopted for other applications (see, for example, [21, 22]). However, it was shown in [23] that whenever a compact set cannot be globally asymptotically stabilized by means of continuous feedback it cannot be *robustly* stabilized by means of discontinuous feedback either – in the sense that there exists arbitrarily small noise that prevents the state of the system from ever leaving unwanted regions of the state space (see also [24]). This led to the development of more sophisticated control strategies that make use of recent results in the domain of hybrid dynamical systems [25, 26]. It was shown in [25] that hybrid systems verifying the so-called *Basic Assumptions* are inherently robust to small measurement noise, making them a suitable approach to address the attitude control problem. Namely, a hybrid control strategy for the global stabilization on $SO(3)$ that makes use of the quaternion representation of rotation was proposed in [27]. More recently, the introduction of *synergistic potential functions* on $SO(3)$ enabled the development of globally stabilizing hybrid feedback laws in terms of the rotation matrix [28].

A natural extension of the attitude control problem is the control of both position and attitude, allowing for the tracking of reference trajectories that evolve on the *special Euclidean group of order 3*, denoted by $SE(3) = \mathbb{R}^3 \times SO(3)$. The literature on this subject is vast and includes tracking control of both fully actuated vehicles [29, 30] and underactuated vehicles [31, 32]. Most notably, the control law proposed in [33] provides a solution to the problem of globally stabilizing the attitude and position of a rigid body that is robust to measurement noise. Nevertheless, most of these works do not delve into the details of reconstructing the state of the system out of sensor measurements. In order to bypass this problem, there was considerable effort put into the development of feedback laws that directly utilize vector measurements to achieve the desired goal [34, 35, 36].

In this paper, we combine the recent developments on the use of synergistic potential functions defined on $SO(3)$ [28] with the landmark-based control solution presented in [34] and [35], to design a hybrid control algorithm that uses the angular velocity, the position of known landmarks and their rate of change to globally asymptotically stabilize the attitude and the position of a rigid-body to a desired reference trajectory. Similarly to [34] and [35], the proposed algorithm does not insist on reconstructing the state, thus the control input can be computed directly from the sensor measurements. On the other hand, we improve the controllers presented in the aforementioned papers, because we consider the problem of trajectory tracking instead of set-point stabilization, we design a controller that provides global asymptotic stability instead of almost global asymptotic stability and, by using a

DOI: 10.1002/rnc

hybrid controller that meets the hybrid basic conditions, we also guarantee that the closed-loop system is robust to small measurement noise.

Sufficient conditions on the geometry of the landmarks enabling the desired goal to be met are provided. In addition, we also provide sufficient conditions for the existence of synergistic potential functions on $SO(3)$, thus complementing the work by [28]. The results presented in this work have direct application to vehicles that can be modelled as fully actuated rigid bodies and use cameras, laser sensors, and other devices that allow the position of given landmarks to be measured. A preliminary version of this work was presented at the *51st Conference on Decision and Control* [37].

The remainder of this paper is organized as follows. In Section 1, we present some of the notational conventions that are used throughout the paper. Section 3 describes the problem setup which is addressed in Section 4. Simulation results are provided in Section 5 so as to demonstrate the capabilities and the performance of the controller. Finally, some concluding remarks are given in Section 6.

2. PRELIMINARIES

2.1. Notation

In this section, we present some of the notation used in the sequel. Column vectors are represented by boldface characters and scalars are represented by regular lowercase characters, for example $\mathbf{v} = \begin{bmatrix} v_1 & v_2 & \dots & v_p \end{bmatrix}^\top$ represents a vector in $\mathbb{R}^p$. Matrices are represented by regular uppercase characters.

We define the vector of ones $\mathbf{1}_p := [1 \;\; 1 \;\; \dots \;\; 1]^\top \in \mathbb{R}^p$, the vector of zeros $\mathbf{0}_p := [0 \;\; 0 \;\; \dots \;\; 0]^\top \in \mathbb{R}^p$, and the canonical basis vector $\mathbf{e}_i \in \mathbb{R}^p$ whose components are equal to 0 except for the i-th component which is equal to 1. Moreover, given $\mathbf{v} \in \mathbb{R}^p$, we define the function $\mathrm{diag} : \mathbb{R}^p \to \mathbb{R}^{p \times p}$ as

$$\mathrm{diag}(\mathbf{v}) := \begin{bmatrix} v_1 & 0 & \dots & 0 \\ 0 & v_2 & \ddots & \vdots \\ \vdots & \ddots & \ddots & 0 \\ 0 & \dots & 0 & v_p \end{bmatrix}.$$

Moreover, we make used of the following notation in this paper:

- The set $\mathbb{R}_{\geq 0} \subset \mathbb{R}$ is the set of all non-negative real numbers;
- $\mathbb{N}_0$ is the set of natural numbers and 0;
- The norm $|.|_{\mathcal{A}} : \mathbb{R}^p \to \mathbb{R}_{\geq 0}$ provides the shortest distance from a point $\mathbf{x} \in \mathbb{R}^p$ to the set $\mathcal{A} \subset \mathbb{R}^p$, i.e., $|\mathbf{x}|_{\mathcal{A}} = \inf_{\mathbf{y} \in \mathcal{A}} |\mathbf{x} - \mathbf{y}|$, where $|.| : \mathbb{R}^p \to \mathbb{R}_{\geq 0}$ denotes the standard Euclidean distance. We make an exception for the Frobenius norm, which we will denote by $|.|_F : \mathbb{R}^{m \times n} \to \mathbb{R}$ and is given by $|A|_F = \sqrt{\langle A, A \rangle}$;
- The symbol $B(\mathbf{x}, r)$ denotes the open ball of radius $r > 0$ around $\mathbf{x} \in \mathbb{R}^p$, i.e., $B(\mathbf{x}, r) := \{\mathbf{y} \in \mathbb{R}^p : |\mathbf{y} - \mathbf{x}| < r\}$;
- A function $\alpha : \mathbb{R}_{\geq 0} \mapsto \mathbb{R}_{\geq 0}$ is a class-$\mathcal{K}_\infty$ function, also written $\alpha \in \mathcal{K}_\infty$, if α is zero at zero, continuous, strictly increasing, and unbounded.

Finally, we introduce some geometry concepts which are mostly used during the description of the problem setup in Section 3.

Definition ([38])
The set of all affine combinations of points in some set $H \subseteq \mathbb{R}^p$ is called the *affine hull* of

DOI: 10.1002/rnc

H, and is given by

$$\mathbf{aff}(H) := \{\mathbf{y} \in \mathbb{R}^p : \mathbf{y} = \sum_{i=0}^{k} \alpha_i \mathbf{x}_i \text{ for some } k \in \mathbb{N}_0, \{\mathbf{x}_i\}_{i\in\{0,1,\ldots,k\}} \subset H, \{\alpha_i\}_{i\in\{0,1,\ldots,k\}} \subset \mathbb{R} \text{ such that } \sum_{i=0}^{k} \alpha_i = 1\}.$$

The *affine dimension* of a set H is the minimum number $k \in \mathbb{N}_0$ of vectors $\{\mathbf{x}_i\}_{i\in\{0,1,\ldots,k\}}$ belonging to H such that $\mathbf{aff}(\{\mathbf{x}_i\}_{i\in\{0,1,\ldots,k\}}) = \mathbf{aff}(H)$. □

Definition ([38])
The *relative interior* of a set $H \subseteq \mathbb{R}^p$, denoted by $\mathbf{relint}(H)$, is its interior relative to $\mathbf{aff}(H)$, and is given by

$$\mathbf{relint}(H) := \{\mathbf{x} \in \mathbb{R}^p : B(\mathbf{x}, r) \cap \mathbf{aff}(H) \subseteq H \text{ for some } r > 0\}.$$ □

Definition ([38])
The *convex hull* of a set $H \subseteq \mathbb{R}^p$, denoted by $\mathbf{conv}(H)$, is given by

$$\mathbf{conv}(H) := \{\mathbf{y} \in \mathbb{R}^p : \mathbf{y} = \theta\mathbf{x}_1 + (1-\theta)\mathbf{x}_2 \text{ for some } \mathbf{x}_1, \mathbf{x}_2 \in H, \theta \in [0,1]\}.$$ □

2.2. Lie Groups

The dynamical systems considered in this paper evolve on $SE(3)$, which motivates the following definitions.

Definition ($SE(3)$)
The Special Euclidean Group of order 3, denoted by $SE(3)$, is the set $\mathbb{R}^3 \times SO(3)$ endowed with product operation $(p_1, \mathcal{R}_1).(p_2, \mathcal{R}_2) = (p_1 + \mathcal{R}_1 p_2, \mathcal{R}_1\mathcal{R}_2)$, where $SO(3)$ denotes the Special Orthogonal Group of order 3, given by the set

$$SO(3) := \{\mathcal{R} \in \mathbb{R}^{3\times 3} : \mathcal{R}^\top\mathcal{R} = \mathbf{I}_3, \det(\mathcal{R}) = 1\}.$$

and the standard matrix multiplication. □

Recalling that a Lie group is a smooth manifold that is also a group, with smooth group multiplication and inverse operations, then it is easy to check that the set of $p \times p$ invertible matrices, denoted by $GL(p)$, is a Lie group under the standard matrix multiplication [39, Example 7.3]. Given $A \in GL(3)$, let $F(A) = A^\top A$. The map F is a smooth submersion onto the space of 3×3 symmetric matrices, therefore its level sets are embedded submanifolds of $GL(3)$ [39, Corollary 5.13]. In particular, the component of level set of $\mathbf{I}_3$ containing the identity is precisely $SO(3)$. Since $SO(3)$ is a subgroup and an embedded submanifold of $GL(3)$, we conclude by [39, Proposition 7.11] that it is a Lie subgroup of $GL(3)$. On the other hand, the map $G : SE(3) \to GL(4)$, given by

$$G(\mathbf{p}, \mathcal{R}) := \begin{bmatrix} \mathcal{R} & \mathbf{p} \\ \mathbf{0}_3^\top & 1 \end{bmatrix},$$

is an injective Lie group homomorphism. Therefore, by [39, Proposition 7.17], we conclude that $SE(3)$ is a Lie subgroup of $GL(4)$. The Lie algebra of a Lie group is defined as the tangent space at the identity together with the Lie bracket operation, given by $\mathrm{ad}_X(Y) = XY - YX$, for any $X, Y \in \mathbb{R}^{p\times p}$ in the algebra (for more details on this topic see [40]).

Definition (Lie Algebra of $SO(3)$)
The Lie Algebra of the $SO(3)$ is denoted by $\mathfrak{so}(3)$ and is given by the set

$$\mathfrak{so}(3) = \{M \in \mathbb{R}^{3\times 3} : M = -M^\top\},$$

together with the Lie bracket operation. □

DOI: 10.1002/rnc

The operator $S : \mathbb{R}^3 \to \mathfrak{so}(3)$ denotes the isomorphism between the algebras $(\mathbb{R}^3, \times)$ and $(\mathfrak{so}(3), \mathrm{ad})$ (with inverse denoted by $S^{-1} : \mathfrak{so}(3) \to \mathbb{R}^3$). It is possible to show that the mapping $S : \mathbb{R}^3 \to \mathfrak{so}(3)$ has the following property: $S(\mathbf{x})\mathbf{y} = \mathbf{x} \times \mathbf{y}$ for any $\mathbf{x}, \mathbf{y} \in \mathbb{R}^3$, therefore it is given by

$$S(\mathbf{x}) := \begin{bmatrix} 0 & -x_3 & x_2 \\ x_3 & 0 & -x_1 \\ -x_2 & x_1 & 0 \end{bmatrix}, \quad S^{-1}\left(\begin{bmatrix} 0 & -x_3 & x_2 \\ x_3 & 0 & -x_1 \\ -x_2 & x_1 & 0 \end{bmatrix}\right) := \mathbf{x}.$$

We introduce the following operator, which is used extensively in the sequel,

$$\begin{aligned} \varphi : \mathbb{R}^{3\times 3} &\to \mathbb{R}^3 \\ A &\mapsto S^{-1}\left(A - A^\top\right), \end{aligned}$$

with the property that for each $A \in \mathbb{R}^{3\times 3}$ and for each $z \in \mathbb{R}^3$:

$$\mathrm{trace}(AS(z)) = z^\top \varphi(A^\top). \tag{1}$$

Moreover, we define the inner product between two matrices as follows

$$\begin{aligned} \langle ., . \rangle : \mathbb{R}^{m\times p} \times \mathbb{R}^{m\times p} &\to \mathbb{R} \\ (A, B) &\mapsto \mathrm{trace}(A^\top B), \end{aligned} \tag{2}$$

which, in the particular case $\mathbf{x}, \mathbf{y} \in \mathbb{R}^p$, is given by $\langle \mathbf{x}, \mathbf{y} \rangle = \mathbf{x}^\top \mathbf{y}$. As outlined in [5, Example 1.4], given a continuously differentiable function over the Riemannian manifold $(SO(3), \langle ., . \rangle)$, $V : SO(3) \to \mathbb{R}$, $\mathcal{R} \in SO(3)$ is a critical point of V if

$$\langle \nabla V(\mathcal{R}), X \rangle = 0, \; \forall \; X \in T_{\mathcal{R}} SO(3), \tag{3}$$

where $T_{\mathcal{R}} SO(3)$ denotes the tangent space to $SO(3)$ at $\mathcal{R}$, and we use the notation

$$\left[\nabla V(\mathcal{R})\right]_{ij} := \frac{\partial V(\mathcal{R})}{\partial \mathcal{R}_{ij}}.$$

By noticing that $T_{\mathcal{R}} SO(3) \cong \{X \in \mathbb{R}^{3\times 3} : X = \mathcal{R}S(\omega) \text{ for some } \omega \in \mathbb{R}^3\}$, using (1) and (2), it follows from (3) that the set of critical points is given by

$$\mathrm{Crit}\; V := \{\mathcal{R} \in SO(3) : \varphi(\mathcal{R}^\top \nabla V(\mathcal{R})) = 0\}.$$

Let $\mathbb{S}^p \subset \mathbb{R}^{p+1}$ denote the p-dimensional sphere, defined by $\mathbb{S}^p := \{\mathbf{x} \in \mathbb{R}^{p+1} : \mathbf{x}^\top \mathbf{x} = 1\}$. With a slight abuse of notation, we define

$$\begin{aligned} \mathcal{R} : \mathbb{S}^2 \times [0, \pi] &\to SO(3) \\ (\theta, \mathbf{u}) &\mapsto e^{\theta S(\mathbf{u})} = \mathbf{I}_3 + \sin(\theta) S(\mathbf{u}) + (1 - \cos(\theta)) S(\mathbf{u})^2, \end{aligned} \tag{4}$$

where $\mathbf{u} \in \mathbb{S}^2$ denotes the axis of rotation and $\theta \in [0, \pi]$ denotes the rotation angle [19]. It is easy to see that $\mathcal{R}(\pi, \mathbf{u}) = \mathcal{R}(\pi, -\mathbf{u})$, therefore the covering map (4) is many-to-one. For more information on the topological issues related to the $SO(3)$ manifold, see [4].

In this paper, we are interested in trajectories evolving on the tangent bundle of $SE(3)$, denoted by $TSE(3)$. The tangent bundle of $SE(3)$ is, by definition, the disjoint union of $T_{(\mathbf{p},\mathcal{R})} SE(3)$ for each $(\mathbf{p}, \mathcal{R}) \in SE(3)$, where $T_{(\mathbf{p},\mathcal{R})} SE(3)$ denotes the tangent space to $SE(3)$ at $(\mathbf{p}, \mathcal{R}) \in SE(3)$, given by

$$\begin{aligned} T_{(\mathbf{p},\mathcal{R})} SE(3) &= \mathbb{R}^3 \times T_{\mathcal{R}} SO(3) \\ &= \{(\mathbf{u}, X) \in \mathbb{R}^3 \times \mathbb{R}^{3\times 3} : X^\top \mathcal{R} = -\mathcal{R}^\top X\}. \end{aligned}$$

Prepared using rncauth.cls
DOI: 10.1002/rnc

It is possible to show that the map

$$\varrho : TSE(3) \to SE(3) \times \mathbb{R}^6$$
$$(\mathbf{p}, \mathcal{R}, \mathbf{u}, X) \mapsto \left(\mathbf{p}, \mathcal{R}, \mathbf{u}, S^{-1}\left(\mathcal{R}^\top X\right)\right),$$

is a diffeomorphism from $TSE(3)$ onto $SE(3) \times \mathbb{R}^6$. Therefore, trajectories evolving on $TSE(3)$ can be identified with trajectories on $SE(3) \times \mathbb{R}^6$.

2.3. Hybrid Systems

In this paper, we make use of recent developments on hybrid systems theory that are described in [25]. Under this framework, a hybrid system $\mathcal{H}$ is defined as

$$\mathcal{H} = \begin{cases} \dot{\boldsymbol{\xi}} \in F(\boldsymbol{\xi}) & \boldsymbol{\xi} \in C \\ \boldsymbol{\xi}^+ \in G(\boldsymbol{\xi}) & \boldsymbol{\xi} \in D \end{cases},$$

where the data (F, C, G, D) is given as follows: the set-valued map $F : \mathbb{R}^p \rightrightarrows \mathbb{R}^p$ is the *flow map* and governs the continuous dynamics (also known as flows) of the hybrid system; the set $C \subset \mathbb{R}^p$ is the *flow set* and defines the set of points where the system is allowed to flow; the set-valued map $G : \mathbb{R}^p \rightrightarrows \mathbb{R}^p$ is the *jump map* and defines the behaviour of the system during jumps; the set $D \subset \mathbb{R}^p$ is the *jump set* and defines the set of points where the system is allowed to jump.

In order to define the concept of solutions to hybrid systems, we need to introduce the concepts of *hybrid time domain* and *hybrid arcs* given next.

Definition ([26, Definition 2.3])
A subset E of $\mathbb{R}_{\geq 0} \times \mathbb{N}_0$ is a compact hybrid time domain if

$$E = \bigcup_{j=0}^{J-1} ([t_j, t_{j+1}], j)$$

for some finite sequence of times $0 \leq t_0 \leq t_1 \leq t_2 \leq \ldots \leq t$. It is a hybrid time domain if for all $(T, J) \in E$, $E \cap ([0, T] \times \{0, 1, \ldots, J\})$ is a compact hybrid time domain.

Definition ([26, Definition 2.4])
A function $\boldsymbol{\xi} : E \to \mathbb{R}^n$ is a hybrid arc if E is a hybrid time domain and if for each $j \in \mathbb{N}_0$, the function $t \mapsto \boldsymbol{\xi}(t, j)$ is locally absolutely continuous on the interval $I_j = \{t : (t, j) \in E\}$.

Equipped with these definitions, we are able to define precisely the solutions to hybrid systems as follows.

Definition ([26, Definition 2.6])
A hybrid arc $\boldsymbol{\xi}$ is a solution to the hybrid system (C, F, D, G) if $\boldsymbol{\xi}(0, 0) \in \overline{C} \cup D$, and

(S1) for all $j \in \mathbb{N}_0$ such that $I_j := \{t : (t, j) \in \operatorname{dom} \boldsymbol{\xi}\}$ has nonempty interior

$$\begin{array}{lll} \boldsymbol{\xi}(t, j) \in C & \text{for all} & t \in \operatorname{int} I_j, \\ \frac{d\boldsymbol{\xi}}{dt}(t, j) \in F(\boldsymbol{\xi}) & \text{for almost all} & t \in I_j; \end{array}$$

(S2) for all $(t, j) \in \operatorname{dom} \boldsymbol{\xi}$ such that $(t, j + 1) \in \operatorname{dom} \boldsymbol{\xi}$,

$$\boldsymbol{\xi}(t, j) \in D,$$
$$\boldsymbol{\xi}(t, j + 1) \in G(\boldsymbol{\xi}(t, j))$$

A solution $\boldsymbol{\xi}$ is maximal if it cannot be extended, that is, the hybrid system has no solution $\boldsymbol{\xi}'$ such that $\operatorname{dom} \boldsymbol{\xi}'$ is a proper subset of $\operatorname{dom} \boldsymbol{\xi}$ and $\boldsymbol{\xi}'$ agrees with $\boldsymbol{\xi}$ for all $(t, j) \in \operatorname{dom} \boldsymbol{\xi}$, and it is *complete* if its domain is unbounded [25, p. 41].

Prepared using rncauth.cls
DOI: 10.1002/rnc

Definition ([26, Definition 3.6])
Consider a hybrid system $\mathcal{H} = (F, C, G, D)$ defined in $\mathbb{R}^p$. Let $\mathcal{A} \subset \mathbb{R}^p$ be closed. The set $\mathcal{A}$ is said to be:

- *Globally Stable* for $\mathcal{H}$ if there exists a function $\alpha \in \mathcal{K}_\infty$ such that for any solution $\boldsymbol{\xi}$ to $\mathcal{H}$, $|\boldsymbol{\xi}(t,j)|_\mathcal{A} \leq \alpha(|\boldsymbol{\xi}(0,0)|_\mathcal{A})$ for all $(t,j) \in \operatorname{dom} \boldsymbol{\xi}$;
- *Globally Attractive* for $\mathcal{H}$ if any complete solution $\boldsymbol{\xi}$ to $\mathcal{H}$ satisfies $\lim_{t+j\to\infty} |\boldsymbol{\xi}(t,j)|_\mathcal{A} = 0$;
- *Globally Asymptotically Stable* (GAS) for $\mathcal{H}$ if it is both globally stable and globally attractive for $\mathcal{H}$.

This paper builds on the results in [41], where synergistic potential functions. For completeness, we include the definition of such functions.

Definition ([41, Definition 1])
A continuously differentiable function $V : SO(3) \to \mathbb{R}_{\geq 0}$ is a *potential function* on $SO(3)$ (with respect to $\mathbf{I}_3$) if $V(\mathcal{R}) > 0$ for all $\mathcal{R} \in SO(3)\backslash\{\mathbf{I}_3\}$ and $V(\mathbf{I}_3) = 0$. The class of potential functions on $SO(3)$ is denoted by $\mathscr{P}$. □

Definition ([41, Definition 2])
Let $Q \subset \mathbb{Z}$ be a finite index set with cardinality N and define $\mu : \mathscr{P}^N \to \mathbb{R}_{\geq 0}$, such that, for each family of potential functions $\mathscr{V} = \{V_q\}_{q\in Q} \in \mathscr{P}^N$,

$$\mu(\mathscr{V}) := \inf_{\substack{q\in Q \\ \mathcal{R}\in \mathrm{Crit}\ V_q\backslash\{\mathbf{I}_3\}}} \max_{p\in Q} \left(V_q(\mathcal{R}) - V_p(\mathcal{R})\right). \tag{5}$$

The family $\mathscr{V} \in \mathscr{P}^N$ is synergistic if there exists $\delta > 0$ such that

$$\mu(\mathscr{V}) > \delta,$$

where we say that $\mathscr{V}$ is synergistic with gap exceeding δ. □

3. PROBLEM SETUP

Given an orthonormal inertial reference frame $\{I\}$ and an orthonormal frame $\{B\}$, which is fixed with respect to a fully actuated rigid body vehicle, the dynamic equations of motion are given by

$$\dot{\mathbf{p}} = \mathbf{v} - S(\boldsymbol{\omega})\mathbf{p}, \tag{6a}$$
$$\dot{\mathcal{R}} = \mathcal{R}S(\boldsymbol{\omega}), \tag{6b}$$
$$\dot{\mathbf{v}} = \frac{\mathbf{f}}{m} - S(\boldsymbol{\omega})\mathbf{v}, \tag{6c}$$
$$\dot{\boldsymbol{\omega}} = \mathbf{J}^{-1}(S(\mathbf{J}\boldsymbol{\omega})\boldsymbol{\omega} + \boldsymbol{\tau}), \tag{6d}$$

where $\mathbf{p} \in \mathbb{R}^3$ denotes the position of $\{B\}$ with respect to $\{I\}$, expressed in $\{B\}$, $\mathcal{R} \in SO(3)$ is the rotation matrix which maps vectors in $\{B\}$ to $\{I\}$, such that $\mathcal{R}\mathbf{p}$ denotes the position of $\{B\}$ with respect to $\{I\}$ expressed in $\{I\}$, $\mathbf{v} \in \mathbb{R}^3$ denotes the linear velocity of $\{B\}$ with respect to $\{I\}$, expressed in $\{B\}$, $\boldsymbol{\omega} \in \mathbb{R}^3$ denotes the angular velocity of $\{B\}$ with respect to $\{I\}$ expressed in $\{B\}$, $\mathbf{f} \in \mathbb{R}^3$ and $\boldsymbol{\tau} \in \mathbb{R}^3$ represent the force and the torque exerted on the rigid body, respectively, $m \in \mathbb{R}$ denotes the mass of the vehicle and $\mathbf{J} \in \mathbb{R}^{3\times 3}$ is its tensor of inertia (a very detailed description on this subject may be found in [42]). A wide range of vehicles can be modelled by the rigid body kinematics presented in (6a), (6b), such as aeroplanes, helicopters, underwater vehicles, and others. Even though these vehicles might not be completely rigid, this approximation is very common and it yields good practical

Prepared using rncauth.cls
DOI: 10.1002/rnc

results. The dynamics (6c), (6d) are valid under the assumption that the vehicle is fully-actuated. Moreover, for the purposes of the application discussed in this paper, we assume that the vehicle is equipped with on-board sensors that retrieve its angular velocity $\boldsymbol{\omega}$ such as gyroscopes, as well as the position and the rate of change, with respect to $\{B\}$, of any number of landmarks whose locations are fixed with respect to $\{I\}$, such as laser sensors.

The position of the i-th landmark with respect to $\{I\}$ (out of a set of $n \in \mathbb{N}$ landmarks) is denoted by $\mathbf{x}_i \in \mathbb{R}^3$ and

$$X := \begin{bmatrix} \mathbf{x}_1 & \mathbf{x}_2 & \dots & \mathbf{x}_n \end{bmatrix} \in \mathbb{R}^{3\times n}$$

is a matrix whose columns are the positions of all the n landmarks. The i-th measurement of the on-board sensors is obtained by means of an affine transformation on $\mathbf{x}_i$, and it is given by

$$\boldsymbol{\ell}_i(\mathcal{R}, \mathbf{p}) := \mathcal{R}^\top \mathbf{x}_i - \mathbf{p}.$$

The landmark measurements can also be collected in a matrix, $L \in \mathbb{R}^{3\times n}$, as follows:

$$L(\mathcal{R}, \mathbf{p}) := \mathcal{R}^\top X - \mathbf{p}\mathbf{1}^\top. \tag{7}$$

In order to reduce the notational burden we refer to $L(\mathcal{R}, \mathbf{p})$ as L in the sequel.

Let $x_d = (\mathbf{p}_d, \mathcal{R}_d, \mathbf{v}_d, \boldsymbol{\omega}_d)(t)$ denote a smooth reference trajectory evolving on $SE(3) \times \mathbb{R}^6$ for all $t \geq 0$ which satisfies the following assumption.

Assumption 1
Let $\pi : TSE(3) \to SE(3)$ denote the canonical projection of $TSE(3)$ onto $SE(3)$. The reference trajectory $t \mapsto x_d(t) := (\mathbf{p}_d(t), \mathcal{R}_d(t), \mathbf{v}_d(t), \boldsymbol{\omega}_d(t))$ is a complete and bounded solution to $\dot{x}_d = f_d(x_d)$ satisfying

$$\frac{d}{dt}\pi(\mathbf{p}_d(t), \mathcal{R}_d(t), \mathbf{v}_d(t), \boldsymbol{\omega}_d(t)) = (\mathbf{v}_d(t) - S(\boldsymbol{\omega}_d(t))\mathbf{p}_d(t), \mathcal{R}_d(t)S(\boldsymbol{\omega}_d(t))),$$

for each $t \geq 0$ and for some continuously differentiable vector field f_d on $TSE(3)$. □

For each $t \geq 0$ one may associate a "desired" reference frame $\{D\}$ whose origin is located at $\mathbf{p}_d(t)$ and whose orthonormal basis consists of the columns of $\mathcal{R}_d(t)$. Moreover, this reference trajectory is associated with reference landmark positions $L_d \in \mathbb{R}^{3\times n}$, which are given by

$$L_d = \mathcal{R}_d^\top X - \mathbf{p}_d\mathbf{1}^\top.$$

The main goal of this paper is to design a control law $(\mathbf{f}, \boldsymbol{\tau}) = \kappa(L, \dot{L}, \boldsymbol{\omega}, x_d)$ as a function of the sensor outputs and the reference trajectory, such that

$$\lim_{t\to\infty} (\widetilde{\mathbf{p}}, \widetilde{\mathcal{R}}, \widetilde{\mathbf{v}}, \widetilde{\boldsymbol{\omega}})(t) = (0, \mathbf{I}_3, 0, 0), \tag{8}$$

with

$$\widetilde{\mathbf{p}} := \mathbf{p} - \mathbf{p}_d, \tag{9a}$$
$$\widetilde{\mathcal{R}} := \mathcal{R}_d\mathcal{R}^\top, \tag{9b}$$
$$\widetilde{\mathbf{v}} := \mathbf{v} - \mathbf{v}_d, \tag{9c}$$
$$\widetilde{\boldsymbol{\omega}} := \boldsymbol{\omega} - \boldsymbol{\omega}_d, \tag{9d}$$

holds regardless of the initial condition. Using (6), one verifies that the dynamics of the error variables are given by

$$\dot{\widetilde{\mathbf{p}}} = \widetilde{\mathbf{v}} - S(\boldsymbol{\omega})\mathbf{p} + S(\boldsymbol{\omega}_d)\mathbf{p}_d, \tag{10a}$$
$$\dot{\widetilde{\mathcal{R}}} = -S(\mathcal{R}_d\widetilde{\boldsymbol{\omega}})\widetilde{\mathcal{R}}, \tag{10b}$$
$$\dot{\widetilde{\mathbf{v}}} = \frac{\mathbf{f}}{m} - S(\boldsymbol{\omega})\mathbf{v} - \dot{\mathbf{v}}_d, \tag{10c}$$
$$\dot{\widetilde{\boldsymbol{\omega}}} = \mathbf{J}^{-1}(S(\mathbf{J}\boldsymbol{\omega})\boldsymbol{\omega} + \boldsymbol{\tau}) - \dot{\boldsymbol{\omega}}_d, \tag{10d}$$

Prepared using rncauth.cls
DOI: 10.1002/rnc

which are equivalent to

$$\dot{\widetilde{\mathbf{p}}} = \widetilde{\mathbf{v}} - S(\widetilde{\boldsymbol{\omega}} + \boldsymbol{\omega}_d)\widetilde{\mathbf{p}} + S(\mathbf{p}_d)\widetilde{\boldsymbol{\omega}}, \tag{11a}$$

$$\dot{\widetilde{\mathcal{R}}} = -S(\mathcal{R}_d\widetilde{\boldsymbol{\omega}})\widetilde{\mathcal{R}}, \tag{11b}$$

$$\dot{\widetilde{\mathbf{v}}} = \mathbf{u}_{\mathbf{v}}, \tag{11c}$$

$$\dot{\widetilde{\boldsymbol{\omega}}} = \mathbf{u}_{\boldsymbol{\omega}}, \tag{11d}$$

using the input transformation

$$\mathbf{f} := m(\dot{\mathbf{v}}_d + S(\boldsymbol{\omega})\mathbf{v} + \mathbf{u}_{\mathbf{v}}), \tag{12a}$$

$$\boldsymbol{\tau} := -S(\mathbf{J}\boldsymbol{\omega})\boldsymbol{\omega} + \mathbf{J}(\dot{\boldsymbol{\omega}}_d + \mathbf{u}_{\boldsymbol{\omega}}). \tag{12b}$$

Therefore, the objective specified in (8) is equivalent to the global asymptotic stabilization of the set

$$\mathcal{A} := \{0\} \times \{\mathbf{I}_3\} \times \{0\} \times \{0\} \subset SE(3) \times \mathbb{R}^6$$

for the error system (11) using the virtual inputs $(\mathbf{u}_{\mathbf{v}}, \mathbf{u}_{\boldsymbol{\omega}})$. The following problem statement summarizes the previous discussions.

Problem 1
Let $\mathfrak{X} := \{\mathbf{x}_1, \mathbf{x}_2, \ldots, \mathbf{x}_n\} \subset \mathbb{R}^3$ denote the (fixed) positions of $n \in \mathbb{N}$ landmarks with respect to $\{I\}$ and let $x_d(t)$ denote a reference trajectory satisfying Assumption 1. Given $\mathfrak{X}$, design a landmark-based hybrid controller $\mathcal{H}_c$, with state q and output $(\mathbf{f}, \boldsymbol{\tau}) = \kappa(L, \dot{L}, \boldsymbol{\omega}, x_d, q)$, where L is given by (7), such that $\mathcal{A} := \{0\} \times \{\mathbf{I}_3\} \times \{0\} \times \{0\}$ is *globally asymptotically stable* for the system (11). □

Remark 1
The rate of change of the position of the landmarks, $\dot{L}$, can be measured by optical flow sensors. However, it might be the case that these measurements are not available. In that situation, these measurements might be estimated by differentiating L or replaced by velocity measurements, since $\dot{L}$ is only used to obtain the velocity of the vehicle in the first place, as shown in Section 4.

In order to achieve this goal, we impose the following conditions on $X \in \mathbb{R}^{3\times n}$.

Assumption 2
The origin of $\{I\}$ belongs to the relative interior of the landmarks' convex hull, i.e., $\{0\} \in \mathbf{relint}\ \mathbf{conv}\{\mathbf{x}_1, \mathbf{x}_2, \ldots, \mathbf{x}_n\}$. □

The assertion in the following lemma provides an equivalence between Assumption 2 and the matrix $X \in \mathbb{R}^{3\times n}$, which is very important in the derivation of the main result in this paper.

Lemma 1 ([34, Proposition 3])
Assumption 2 is satisfied if and only if there exists a vector $\mathbf{a} = \begin{bmatrix} a_1 & a_2 & \ldots & a_n \end{bmatrix}^\top$ such that $X\mathbf{a} = 0$, $\mathbf{1}^\top\mathbf{a} = 1$, and $a_j > 0$ for all $j \in \{1, 2, \ldots, n\}$. □

For reasons that will become clearer in Section 4 when we discuss the control strategy, another important assumption on the landmarks geometry relates to their relative positioning.

Assumption 3
Given $\mathbf{a} \in \mathbb{R}^n$ satisfying the conditions of Lemma 1, $XD_aX^\top$ is positive definite with distinct eigenvalues, where $D_a := \mathrm{diag}(\mathbf{a})$. □

Remark 2
Under Assumptions 2 and 3 it is possible to invert the relation (7) in order to find $\mathcal{R}$ and $\mathbf{p}$ out of the sensor measurements. In particular, this would require the computation of the

DOI: 10.1002/rnc

pseudo-inverse of X. The controller proposed in this paper does not require such operations since it uses directly the landmark measurements L, thus saving computational resources and preventing pernicious error scaling from vector noise onto the resolved attitude (cf. [43, p. 1]).

In order to draw some intuition out of Assumptions 2 and 3 one may compare the properties of the landmark setup to the properties of a system of point mass particles. Consider that the particle located at $x_j \in \mathbb{R}^3$ has mass a_j, then it is easy to check that Assumption 2 requires the inertial reference frame to be located at the center of mass. It is also possible to verify that the tensor of inertia of this system of particles is given by $P := \mathrm{trace}(XD_aX^\top)\mathbf{I}_3 - XD_aX^\top$. Assumption 3 implies that the eigenvalues of P are distinct and therefore the system of particles is *anisotropic* [44].

To conclude our analysis on the implications of Assumptions 2 and 3 over the geometry of the landmark constellation, we prove in Lemma 2 that, whenever the landmarks are coplanar, Assumption 3 cannot be satisfied. This straightforward lemma shows that, under the given assumptions, coplanar landmark configurations are not allowed. In particular, any configuration with less than 4 landmarks is not allowed, so we are imposing additional constraints with respect to the results in [34].

Lemma 2
Let $\mathfrak{X} = \{\mathbf{x}_1, \mathbf{x}_2, \ldots, \mathbf{x}_n\} \subset \mathbb{R}^3$ be a set of $n \in \mathbb{N}$ landmarks, fixed with respect to $\{I\}$, satisfying Assumption 2. If the dimension of $\mathbf{aff}(\mathfrak{X})$ is 2, then Assumption 3 is not satisfied.

Proof
Assume that the dimension of $\mathbf{aff}(\mathfrak{X})$ is $n \in \mathbb{N}_0$. Since the set of landmarks $\mathfrak{X}$ satisfies Assumption 2, there exist n linearly independent vectors in $\mathfrak{X}$ or, equivalently, $X = \begin{bmatrix}\mathbf{x}_1 & \mathbf{x}_1 & \ldots & \mathbf{x}_n\end{bmatrix}$ has rank n. If the landmarks are coplanar, then the dimension of $\mathbf{aff}(\mathfrak{X})$ is 2 and, consequently, $\mathrm{rank}(X) = 2$. Then there exists $\mathbf{b} \in \mathbb{R}^3$ such that $X^\top \mathbf{b} = \mathbf{0}_n$ (this can be checked using the singular value decomposition of X), which implies that $XD_aX^\top$ has one zero eigenvalue. This fact implies that Assumption 3 is not satisfied. □

Other landmark geometries must be tested against the assumptions provided in this section in a case-by-case basis. Figure 1 illustrates the physical setup, where the configuration of the body frame $\{B\}$ is shown as well as the inertial reference frame $\{I\}$, the desired configuration of the body frame $\{D\}$ and four landmarks whose positions are the columns of the matrix

$$X = \begin{bmatrix}\mathbf{x}_1 & \mathbf{x}_2 & \mathbf{x}_3 & \mathbf{x}_4\end{bmatrix} := \begin{bmatrix} 1 & -1 & 0 & 0 \\ 0 & 0 & -0.5 & 0.5 \\ -1 & -1 & 1 & 1 \end{bmatrix}. \tag{13}$$

For this particular geometry, we have that $X\mathbf{a} = 0$ for $\mathbf{a} = 0.25\,\mathbf{1}$, thus satisfying Assumption 2 and, the eigenvalues of $XD_aX^\top \in \mathbb{R}^{3\times 3}$ are $\lambda_1 = 1$, $\lambda_2 = 0.5$ and $\lambda_3 = 0.125$, thus meeting Assumption 3. This landmark configuration will be used in Section 5 for simulation purposes.

In the next section, we develop a hybrid control strategy that solves Problem 1.

4. GLOBAL STABILIZATION ON $SE(3) \times \mathbb{R}^6$ BY HYBRID OUTPUT FEEDBACK

In this section, we apply the ideas of using synergistic potential functions for attitude control of a fully actuated rigid body described in [41] to solve Problem 1. Synergistic potential functions on $SO(3)$ (see Definition 2.3) allow for derivation of a class of hybrid controllers that is suitable for the landmark-based control of a fully actuated rigid body. Although we follow very closely the solution for global *asymptotic* stabilization in $SO(3) \times \mathbb{R}^3$ presented in [41], there are some key differences: i) we provide sufficient conditions for the existence

Prepared using rncauth.cls
DOI: 10.1002/rnc

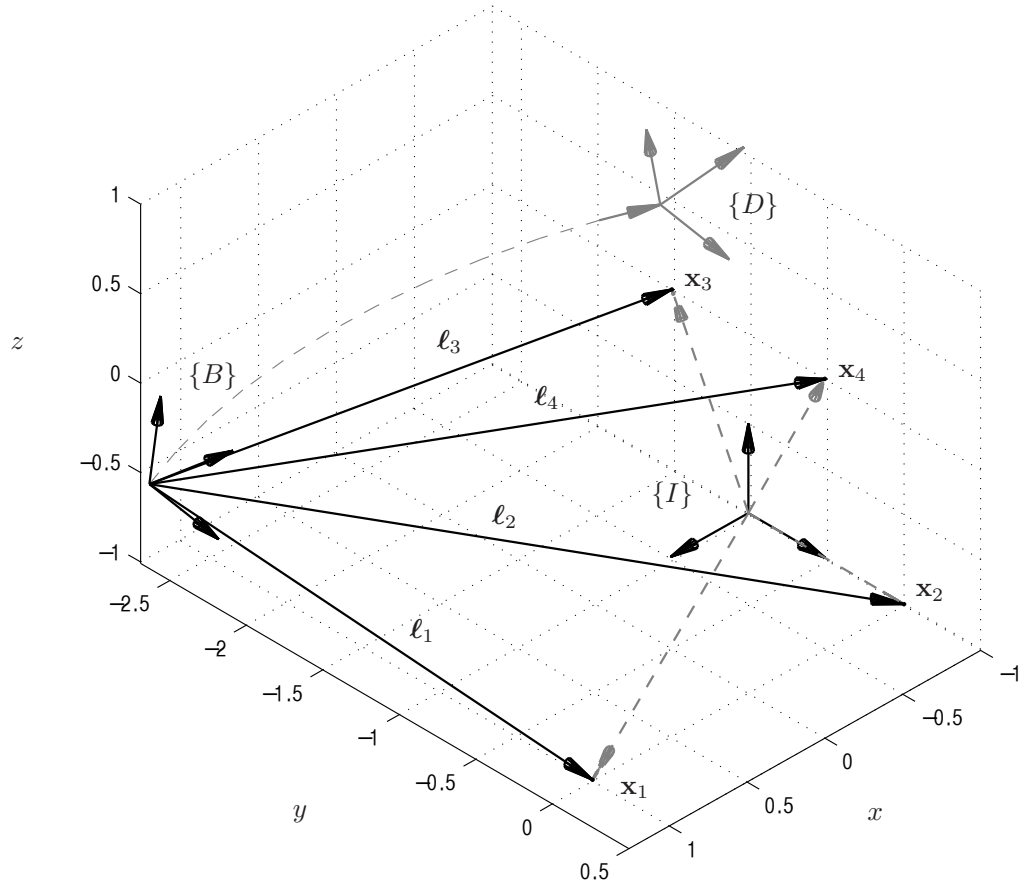

Figure 1. An arbitrary configuration of the body fixed frame $\{B\}$ relative to the inertial reference frame $\{I\}$ and the geometry of the four landmarks used in the simulations presented in Section 5. The symbol $\{D\}$ represents the desired configuration of the body frame.

of a family of synergistic potential functions on $SO(3)$; ii) we extend the problem of global stabilization on $SO(3) \times \mathbb{R}^3$ to that of global stabilization on $SE(3) \times \mathbb{R}^6$; iii) the control law we present does not require attitude estimation because landmark-based information is used directly.

In Section 4.1 we design a feedback law as a function of the state that globally asymptotically stabilizes $\mathcal{A}$, under the assumption that there exists a family of synergistic potential functions on $SO(3)$ with gap exceeding δ. In Section 4.2, we provide sufficient conditions for the existence of such a family of functions and in Section 4.3 we show that the controller can be re-written in terms of the sensor measurements.

Prepared using rncauth.cls
DOI: 10.1002/rnc

4.1. Global Stabilization on $SE(3) \times \mathbb{R}^6$ by State Feedback

Consider the hybrid control law

$$\mathbf{u}_{\boldsymbol{\omega}} := k_{\mathcal{R}} \mathcal{R}_d^\top \widetilde{\mathcal{R}} \varphi(\widetilde{\mathcal{R}}^\top \nabla V_q(\widetilde{\mathcal{R}})) - k_{\boldsymbol{\omega}} \widetilde{\boldsymbol{\omega}} + k_{\mathbf{p}} S(\mathbf{p}_d) \widetilde{\mathbf{p}}, \tag{14a}$$

$$\mathbf{u}_{\mathbf{v}} := -k_{\mathbf{p}} \widetilde{\mathbf{p}} - k_{\mathbf{v}} \widetilde{\mathbf{v}}, \tag{14b}$$

where $k_{\mathcal{R}}, k_{\boldsymbol{\omega}}, k_{\mathbf{p}}, k_{\mathbf{v}} \in \mathbb{R}$, $q \in Q \subset \mathbb{Z}$ is a logic variable, which has continuous dynamics given by $\dot{q} = 0$, and V_q is an element of a family of synergistic potential functions on $SO(3)$ with gap exceeding $\delta > 0$, which is given by $\mathscr{V} := \{V_q\}_{q \in Q}$. This logic variable enables changing the function V_q used in (14), according to the definition of the hybrid system given below

$$\textbf{State: } x = (\widetilde{\mathbf{p}}, \widetilde{\mathcal{R}}, \widetilde{\mathbf{v}}, \widetilde{\boldsymbol{\omega}}, q, \mathbf{p}_d, \mathcal{R}_d, \mathbf{v}_d, \boldsymbol{\omega}_d) \tag{15a}$$

$$\textbf{Flow Map: } F(x) = \begin{pmatrix} \widetilde{\mathbf{v}} - S(\widetilde{\boldsymbol{\omega}} + \boldsymbol{\omega}_d)\widetilde{\mathbf{p}} + S(\mathbf{p}_d)\widetilde{\boldsymbol{\omega}} \\ -S(\mathcal{R}_d \widetilde{\boldsymbol{\omega}})\widetilde{\mathcal{R}} \\ \mathbf{u}_{\mathbf{v}} \\ \mathbf{u}_{\boldsymbol{\omega}} \\ 0 \\ f_d(\mathbf{p}_d, \mathcal{R}_d, \mathbf{v}_d, \boldsymbol{\omega}_d) \end{pmatrix}, \forall x \in C \tag{15b}$$

$$\textbf{Flow Set: } C = \{x \in SE(3) \times \mathbb{R}^6 \times Q \times SE(3) \times \mathbb{R}^6 : V_q(\widetilde{\mathcal{R}}) - \rho(\widetilde{\mathcal{R}}) \leq \delta\} \tag{15c}$$

Jump Map:

$$G(x) = \{(\widetilde{\mathbf{p}}, \widetilde{\mathcal{R}}, \widetilde{\mathbf{v}}, \widetilde{\boldsymbol{\omega}})\} \times \{q' \in Q : V_{q'}(\widetilde{\mathcal{R}}) = \rho(\widetilde{\mathcal{R}})\} \times \{(\mathbf{p}_d, \mathcal{R}_d, \mathbf{v}_d, \boldsymbol{\omega}_d)\}, \forall x \in D \tag{15d}$$

$$\textbf{Jump Set: } D = \{x \in SE(3) \times \mathbb{R}^6 \times Q \times SE(3) \times \mathbb{R}^6 : V_q(\widetilde{\mathcal{R}}) - \rho(\widetilde{\mathcal{R}}) \geq \delta\}. \tag{15e}$$

where $\rho : SO(3) \to \mathbb{R}_{\geq 0}$ is the function defined as

$$\rho(\mathcal{R}) = \min_{q \in Q} V_q(\mathcal{R}).$$

In the next theorem we prove that the set

$$\mathcal{A}_{\mathcal{H}} := \mathcal{A} \times Q \times SE(3) \times \mathbb{R}^6, \tag{16}$$

is globally asymptotically stable for (15).

Theorem 3
Let Assumption 1 be satisfied. Given a family of synergistic potential functions on $SO(3)$, $\mathscr{V} = \{V_q\}_{q \in Q} \in \mathscr{P}^N$, with gap exceeding δ, for any $k_{\mathcal{R}}, k_{\boldsymbol{\omega}}, k_{\mathbf{p}}, k_{\mathbf{v}} > 0$, the set (16) is GAS for the hybrid system (15).

Before presenting the proof, let us recall given a function $f : \mathbb{R}^p \to \mathbb{R}^m$ and a set $Y \subset \mathbb{R}^m$, the *pre-image of* Y *by* f is given by $f^{-1}(Y) := \{x \in \mathbb{R}^p : f(x) \in Y\}$.

Proof of Theorem 3:
The desired result follows from invariance principles for hybrid systems, namely [26, Theorem 8.2]. In order to use this result, we prove that the system is nominally well-posed by showing that it meets the hybrid basic conditions [26, Assumption 6.5], we prove that solutions to the system are precompact (complete and bounded) and we construct a continuously differentiable function V, whose growth is bounded on compact sets.

Let $\phi(\widetilde{\mathcal{R}}, q) := V_q(\widetilde{\mathcal{R}}) - \rho(\widetilde{\mathcal{R}})$ and let $\Delta := \{y \in \mathbb{R} : y \leq \delta\}$. We may rewrite the flow set as follows:

$$C = \{x \in SE(3) \times \mathbb{R}^6 \times Q \times SE(3) \times \mathbb{R}^6 : \phi(\widetilde{\mathcal{R}}, q) \leq \delta\}.$$

Notice that $C = \phi^{-1}(\Delta)$ and that ϕ is a continuous function. Since the pre-image of a closed set by a continuous function is closed ([45, Lemma 2.7]), we have that C is closed. From similar arguments it follows that D is closed. By Assumption 1, it follows that (15b)

Prepared using rncauth.cls
DOI: 10.1002/rnc

is a single-valued smooth function, therefore it is outer-semicontinuous, locally bounded and convex. The jump map is outer-semicontinuous if and only if $D \times G(D)$ is closed ([26, Lemma 5.10]). Notice that the jump map changes the logic variable but not the states, therefore $G(D)$ is closed and $G(x)$ is locally bounded for each $x \in D$. Since D is closed, we conclude that the jump map is outer-semicontinuous.

Consider the following continuous function

$$V(x) := k_{\mathcal{R}} V_q(\widetilde{\mathcal{R}}) + \frac{1}{2}\widetilde{\boldsymbol{\omega}}^\top \widetilde{\boldsymbol{\omega}} + \frac{k_{\mathbf{p}}}{2}\widetilde{\mathbf{p}}^\top \widetilde{\mathbf{p}} + \frac{1}{2}\widetilde{\mathbf{v}}^\top \widetilde{\mathbf{v}}.$$

It is possible to verify that V is positive-definite relative to $\mathcal{A}_{\mathcal{H}}$ and that its time derivative is given by

$$\begin{aligned}\langle \nabla V(x), F(x)\rangle = k_{\mathcal{R}}\langle \nabla V_q(\widetilde{\mathcal{R}}), -S(\mathcal{R}_d\widetilde{\boldsymbol{\omega}})\widetilde{\mathcal{R}}\rangle + \widetilde{\boldsymbol{\omega}}^\top \mathbf{u}_{\boldsymbol{\omega}} + k_{\mathbf{p}}\widetilde{\mathbf{p}}^\top(\widetilde{\mathbf{v}} \\ - S(\widetilde{\boldsymbol{\omega}} + \boldsymbol{\omega}_d)\widetilde{\mathbf{p}} + S(\mathbf{p}_d)\widetilde{\boldsymbol{\omega}}) + \widetilde{\mathbf{v}}^\top \mathbf{u}_{\mathbf{v}}.\end{aligned} \tag{17}$$

Using (2) and $\operatorname{trace}(A^\top B) = \operatorname{trace}(BA^\top)$ we obtain from (17) the following expression

$$\begin{aligned}\langle \nabla V(x), F(x)\rangle = -k_{\mathcal{R}} \operatorname{trace}(\widetilde{\mathcal{R}} \nabla V_q(\widetilde{\mathcal{R}})^\top S(\mathcal{R}_d\widetilde{\boldsymbol{\omega}})) + \widetilde{\boldsymbol{\omega}}^\top \mathbf{u}_{\boldsymbol{\omega}} + k_{\mathbf{p}}\widetilde{\mathbf{p}}^\top(\widetilde{\mathbf{v}} \\ - S(\widetilde{\boldsymbol{\omega}} + \boldsymbol{\omega}_d)\widetilde{\mathbf{p}} + S(\mathbf{p}_d)\widetilde{\boldsymbol{\omega}}) + \widetilde{\mathbf{v}}^\top \mathbf{u}_{\mathbf{v}}.\end{aligned}$$

Using the relations (1), $\mathcal{R}^\top = \mathcal{R}^{-1}$ and $\mathcal{R}\varphi(A) = \varphi(\mathcal{R}A\mathcal{R}^\top)$, valid for any $\mathcal{R} \in SO(3)$, we obtain

$$\begin{aligned}\langle \nabla V(x), F(x)\rangle = -k_{\mathcal{R}}\widetilde{\boldsymbol{\omega}}^\top \mathcal{R}_d^\top \widetilde{\mathcal{R}}\varphi(\widetilde{\mathcal{R}}^\top \nabla V_q(\widetilde{\mathcal{R}})) + \widetilde{\boldsymbol{\omega}}^\top \mathbf{u}_{\boldsymbol{\omega}} + k_{\mathbf{p}}\widetilde{\mathbf{p}}^\top(\widetilde{\mathbf{v}} \\ - S(\widetilde{\boldsymbol{\omega}} + \boldsymbol{\omega}_d)\widetilde{\mathbf{p}} + S(\mathbf{p}_d)\widetilde{\boldsymbol{\omega}}) + \widetilde{\mathbf{v}}^\top \mathbf{u}_{\mathbf{v}}.\end{aligned}$$

Replacing (14) and $\widetilde{\mathbf{p}}^\top S(\widetilde{\boldsymbol{\omega}} + \boldsymbol{\omega}_d)\widetilde{\mathbf{p}} = 0$ into (17) yields

$$\langle \nabla V(x), F(x)\rangle = -k_{\boldsymbol{\omega}}|\widetilde{\boldsymbol{\omega}}|^2 - k_{\mathbf{v}}|\widetilde{\mathbf{v}}|^2 + k_{\mathbf{p}}(\widetilde{\boldsymbol{\omega}}^\top S(\mathbf{p}_d)\widetilde{\mathbf{p}} + \widetilde{\mathbf{p}}^\top S(\mathbf{p})\widetilde{\boldsymbol{\omega}}). \tag{18}$$

Replacing $\widetilde{\boldsymbol{\omega}}^\top S(\mathbf{p}_d)\widetilde{\mathbf{p}} = -\widetilde{\mathbf{p}}^\top S(\mathbf{p}_d)\widetilde{\boldsymbol{\omega}}$ into (18) yields

$$\langle \nabla V(x), F(x)\rangle = -k_{\boldsymbol{\omega}}|\widetilde{\boldsymbol{\omega}}|^2 - k_{\mathbf{v}}|\widetilde{\mathbf{v}}|^2. \tag{19}$$

Moreover, we have that

$$V(x) - V(G(x)) \geq \delta,\ \forall x \in D, \tag{20}$$

by the definition of D and $G(x)$. Let

$$u_c(x) := \begin{cases} -k_{\boldsymbol{\omega}}|\widetilde{\boldsymbol{\omega}}|^2 - k_{\mathbf{v}}|\widetilde{\mathbf{v}}|^2,\ \forall x \in C \\ -\infty, \text{ otherwise}\end{cases},$$

and

$$u_d(x) := \begin{cases} -\delta,\ \forall x \in D \\ -\infty, \text{ otherwise}\end{cases}.$$

In (20) and (19), we have shown that the growth of V along solutions to (15) is bounded by u_c,u_d on $SE(3) \times \mathbb{R}^6 \times Q \times SE(3) \times \mathbb{R}^6$. This result and Assumption 1 imply that solutions to (15) are complete and bounded. It follows from [26, Theorem 8.2] that solutions to (15) converge to the largest weakly invariant subset of $\overline{u_c^{-1}(0)} = \{x \in SE(3) \times \mathbb{R}^6 \times Q \times SE(3) \times \mathbb{R}^6 : \widetilde{\mathbf{v}} = \widetilde{\boldsymbol{\omega}} = 0\} \cap C$. From the definition of the flow map, and from the relations

$$\begin{aligned}\dot{\widetilde{\mathbf{v}}} &\equiv \widetilde{\mathbf{v}} \equiv 0, \\ \dot{\widetilde{\boldsymbol{\omega}}} &\equiv \widetilde{\boldsymbol{\omega}} \equiv 0,\end{aligned}$$

Prepared using rncauth.cls
DOI: 10.1002/rnc

we have that

$$\mathcal{R}_d^\top \widetilde{\mathcal{R}} \varphi(\widetilde{\mathcal{R}} \nabla V_q(\widetilde{\mathcal{R}})) = 0$$
$$\widetilde{\mathbf{p}} = 0.$$

From the relations $\mathcal{R}_d^\top \widetilde{\mathcal{R}} \varphi(\widetilde{\mathcal{R}}^\top \nabla V_q(\widetilde{\mathcal{R}})) = 0 \iff \varphi(\widetilde{\mathcal{R}}^\top \nabla V_q(\widetilde{\mathcal{R}})) = 0 \iff \widetilde{\mathcal{R}} \in \operatorname{Crit} V_q$ we conclude that the largest invariant set of $\underline{u_c^{-1}}(0)$ is a subset of $\{0\} \times \operatorname{Crit} V_q \times \{0\} \times \{0\} \times Q \times SE(3) \times \mathbb{R}^6 \cap C$. Since $\mathscr{V}$ is synergistic with gap exceeding δ, using [28, Lemma 6], we have that $\operatorname{Crit} V_q \cap \{\widetilde{\mathcal{R}} \in SO(3) : V_q(\widetilde{\mathcal{R}}) - \rho(\widetilde{\mathcal{R}}) \leq \delta\} = \{\mathbf{I}_3\}$, therefore $\{0\} \times \operatorname{Crit} V_q \times \{0\} \times \{0\} \times Q \times SE(3) \times \mathbb{R}^6 \cap C = \{0\} \times \{\mathbf{I}_3\} \times \{0\} \times \{0\} \times Q \times SE(3) \times \mathbb{R}^6 = \mathcal{A}_\mathcal{H}$ and we conclude that $\mathcal{A}_\mathcal{H}$ is globally attractive. Since V is positive-definite relative to $\mathcal{A}_\mathcal{H}$ and non-increasing along solutions to (15), then $\mathcal{A}_\mathcal{H}$ is globally stable for (15). It follows that $\mathcal{A}_\mathcal{H}$ is globally asymptotically stable for (15). □

Remark 4
Notice that $\mathbf{u_v}$, defined in (14), depends on the position error, thus coupling the position error and the attitude error subsystems. If, instead of the trajectory tracking problem that is addressed in this paper, we were to consider the point stabilization problem, then it would be possible to decouple the attitude and the position subsystems using a strategy similar to [35].

Notice that the results presented in Theorem 3 partially solve Problem 1 because global asymptotic stabilization of $\mathcal{A}_\mathcal{H}$ for the error system is guaranteed using the state feedback laws (14) (assuming that there exists a family of synergistic potential functions on $SO(3)$ with gap exceeding $\delta > 0$). However, these feedback laws define the virtual control inputs $(\mathbf{u_v}, \mathbf{u_\omega})$ instead of $(\mathbf{f}, \boldsymbol{\tau})$ and it is not clear at this point whether they can be rewritten as a function of the sensor measurements. Nevertheless, the control law for the real inputs $(\mathbf{f}, \boldsymbol{\tau})$ can be computed from (14), using (12), as follows

$$\mathbf{f} = m(\dot{\mathbf{v}}_d + S(\boldsymbol{\omega})\mathbf{v} - k_\mathbf{v}\tilde{\mathbf{v}} - k_\mathbf{p}\tilde{\mathbf{p}}), \tag{21a}$$
$$\boldsymbol{\tau} = -S(\mathbf{J}\boldsymbol{\omega})\boldsymbol{\omega} + \mathbf{J}(\dot{\boldsymbol{\omega}}_d + k_\mathcal{R}\mathcal{R}^\top \varphi(\widetilde{\mathcal{R}}^\top \nabla V_q(\widetilde{\mathcal{R}})) - k_{\boldsymbol{\omega}}\tilde{\boldsymbol{\omega}} + k_\mathbf{p} S(\mathbf{p}_d)\tilde{\mathbf{p}}). \tag{21b}$$

In the sequel we show that (21) can be written as a function of the sensor measurements using a particular family of synergistic potential functions on $SO(3)$ described in the next section.

4.2. A Family of Synergistic Potential Function on $SO(3)$

Let us define the *modified trace function*, given by

$$P_M(\mathcal{R}) := \operatorname{trace}\left((\mathbf{I}_3 - \mathcal{R})M\right), \tag{22}$$

where $M \in \mathbb{R}^{3\times 3}$ is positive definite. This function corresponds to the Frobenius norm of $(\mathbf{I}_3 - \mathcal{R})M^{\frac{1}{2}}$ squared, therefore it is a standard potential function on $SO(3)$. If, in addition, the matrix $M \in \mathbb{R}^{3\times 3}$ possesses distinct eigenvalues, then the number of critical points is four, with one of them being $\{\mathbf{I}_3\}$ (cf. [2]). However, it was proved in [41, Theorem 4] that any family of modified trace functions is not synergistic. On the other hand, it was shown by example that two modified trace functions can become synergistic by *angular warping*, that is, there exists $\delta > 0$ such that $\mu(\mathscr{V}) \geq \delta$ for $\mathscr{V} = \{V_q\}_{q\in\{1,2\}}$ with

$$V_q(\mathcal{R}) := P_{M_q}(\mathcal{T}_q(\mathcal{R})) \tag{23}$$

$$\mathcal{T}_q(\mathcal{R}) := e^{k_q P_{M_q}(\mathcal{R}) S(\mathbf{u}_q)}\mathcal{R} \tag{24}$$

where $\mathcal{T}_q : SO(3) \to SO(3)$ is a diffeomorphism in $SO(3)$ as long as

$$\sqrt{2}k_q \max_{\widetilde{\mathcal{R}}\in SO(3)} \|\nabla P_M(\widetilde{\mathcal{R}})\|_F < 1.$$

DOI: 10.1002/rnc

The function $\mathcal{T}(.)$ corresponds to a rotation of $\mathcal{R} \in SO(3)$ by an amount $k_q P_M(\mathcal{R}) \in \mathbb{R}$ around the axis $\mathbf{u}_q \in \mathbb{S}^2$. Below, in Theorem 5, we establish that, given a symmetric, positive-definite matrix $M \in \mathbb{R}^{3\times 3}$ with distinct eigenvalues, there always exists a family of two potential functions on $SO(3)$ that is synergistic with gap exceeding δ. This theorem proves that the results in [41] are not a product of chance and, additionally, it provides a constructive method to devise synergistic potential functions on $SO(3)$.

Theorem 5
Let $Q := \{1, 2\}$ and $\mathbf{u} \in \mathbb{S}^2$. Given any symmetric, positive-definite matrix $M \in \mathbb{R}^{3\times 3}$ with distinct eigenvalues and $k > 0$ satisfying

$$\sqrt{2}k \max_{\mathcal{R}\in SO(3)} \|\nabla P_{M_q}(\mathcal{R})\|_F < 1 \tag{25}$$

with $M_q = M$ for each $q \in Q$, then the family $\mathscr{V} := \{V_q(\mathcal{R})\}_{q\in Q}$, where V_q is given by (23), defines a family of potential functions on $SO(3)$. Let $\lambda_i \in \mathbb{R}$ and $\mathbf{v}_i \in \mathbb{S}^2$ for each $i \in \{1, 2, 3\}$ denote the eigenvalues and the associated eigenvectors of the matrix M, if $\mathbf{u} = \mathbf{u}_1 = \mathbf{u}_2$ and $k = k_1 = -k_2$ then $\mathscr{V}$ is synergistic with gap exceeding δ for some $\delta > 0$ if and only if

$$\begin{cases} \lambda_1(1 - (\mathbf{u}^\top \mathbf{v}_1)^2) + \lambda_2(1 - (\mathbf{u}^\top \mathbf{v}_2)^2) > \lambda_3(1 - (\mathbf{u}^\top \mathbf{v}_3)^2) \\ \lambda_1(1 - (\mathbf{u}^\top \mathbf{v}_1)^2) + \lambda_3(1 - (\mathbf{u}^\top \mathbf{v}_3)^2) > \lambda_2(1 - (\mathbf{u}^\top \mathbf{v}_2)^2) \\ \lambda_2(1 - (\mathbf{u}^\top \mathbf{v}_2)^2) + \lambda_3(1 - (\mathbf{u}^\top \mathbf{v}_3)^2) > \lambda_1(1 - (\mathbf{u}^\top \mathbf{v}_1)^2). \end{cases} \tag{26}$$

Proof
See Appendix A. □

Corollary 1
Given any symmetric, positive-definite matrix $M \in \mathbb{R}^{3\times 3}$ with eigenvectors $v_i \in \mathbb{S}^2$ with associated eigenvalues $\lambda_i \in \mathbb{R}$ for $i \in \{1, 2, 3\}$, satisfying $\lambda_1 > \lambda_2 > \lambda_3$ and $k > 0$ satisfying (25) with $M_q = M$ for each $q \in Q := \{1, 2\}$, then there exists $\delta > 0$ such that the family $\mathscr{V} := \{V_q(\mathcal{R})\}_{q\in Q}$, where V_q is given by (23), is *synergistic with gap exceeding* δ for the selection of parameters $k = k_1 = -k_2$, $\mathbf{u}_1 = \mathbf{u}_2 = \mathbf{u}$ where

$$\mathbf{u} := \cos\theta \mathbf{v}_1 + \sin\theta \mathbf{v}_2 + \sin\theta \mathbf{v}_3, \tag{27}$$

and

$$\theta \in \left(\arcsin\left(\sqrt{\frac{\lambda_2 - \lambda_3}{\lambda_1 + \lambda_2}} \right), \arcsin\left(\sqrt{\frac{\lambda_3 + \lambda_2}{\lambda_1 + \lambda_2}} \right) \right). \tag{28}$$

Proof
Replacing (27) into (26) yields the following after some algebraic manipulation

$$\begin{cases} \sin^2\theta > \frac{\lambda_3 - \lambda_2}{\lambda_1 - \lambda_2} \\ \sin^2\theta > \frac{\lambda_2 - \lambda_3}{\lambda_1 + \lambda_2} \\ \sin^2\theta < \frac{\lambda_3 + \lambda_2}{\lambda_1 + \lambda_2}. \end{cases}.$$

The first inequality holds trivially because we have assumed $\lambda_1 > \lambda_2 > \lambda_3$. Since

$$\frac{\lambda_2 - \lambda_3}{\lambda_1 + \lambda_2} < \frac{\lambda_3 + \lambda_2}{\lambda_1 + \lambda_2},$$

we conclude that for any θ satisfying (28), the second and the third inequalities of (26) are satisfied, thus, by Theorem 5, $\mathscr{V}$ is synergistic with gap exceeding δ for some $\delta > 0$. □

In Theorem 3, we prove that the set (16) is globally asymptotically stable for the hybrid system (15) assuming that there exists a family of synergistic potential functions on $SO(3)$ with gap exceeding δ. However, in Theorem 5, we provide sufficient conditions for the

Prepared using rncauth.cls
DOI: 10.1002/rnc

existence of such families of functions, therefore, as long as these conditions are met, we can build a controller that achieves the desired goal. This is summarized in the following corollary.

Corollary 2
Let Assumption 1 be satisfied. Given any symmetric, positive-definite matrix $M \in \mathbb{R}^{3\times 3}$ with distinct eigenvalues and $k > 0$ satisfying (25), there exists a family of synergistic potential functions on $SO(3)$ with gap exceeding $\delta > 0$ such that, for any $k_{\mathcal{R}}, k_{\boldsymbol{\omega}}, k_{\mathbf{p}}, k_{\mathbf{v}} > 0$, the set (16) is globally asymptotically stable for the hybrid system (15).

Proof
The existence of a family of synergistic potential functions on $SO(3)$ follows from Theorem 5. From [41, Theorem 6], we obtain the following expression

$$\varphi(\widetilde{\mathcal{R}}^\top \nabla V_q(\widetilde{\mathcal{R}})) = -\Theta(\widetilde{\mathcal{R}}, q)^\top \varphi(\mathcal{T}_q(\widetilde{\mathcal{R}})M) \tag{29}$$

with

$$\Theta(\widetilde{\mathcal{R}}, q) = \mathbf{I}_3 + k_q \widetilde{\mathcal{R}}^\top \mathbf{u}_q \varphi(\widetilde{\mathcal{R}}M)^\top \widetilde{\mathcal{R}}. \tag{30}$$

Replacing the aforementioned expressions into (14), we obtain a hybrid control law which achieves global reference tracking using the family of synergistic potential functions on $SO(3)$ given by (23). Then, the result follows directly from Theorem 3. □

4.3. Global Stabilization on $SE(3) \times \mathbb{R}^6$ by Hybrid Output Feedback

In order to solve Problem 1, we need to rewrite the controller as a function of the sensor measurements, which amounts to rewriting the flow set (15c), the jump map (15d), the jump set (15e) and the control law (21) as functions of L, $\dot{L}$ and $\boldsymbol{\omega}$. To this end, notice that, using $M := XD_aX^\top$ it is possible to rewrite the modified trace function as follows

$$P_M(\widetilde{\mathcal{R}}) = \frac{1}{2}\operatorname{trace}((L - L_d)(\mathbf{I}_n - \mathbf{a}\mathbf{1}^\top)D_a(\mathbf{I}_n - \mathbf{1}\mathbf{a}^\top)(L^\top - L_d^\top)).$$

Since we can write $P_M(\widetilde{\mathcal{R}})$ as a function of the landmarks, with a slight abuse of notation, we refer to this function as $P_M(L)$ in the sequel. Similarly, it is also possible to show that $V_q(\widetilde{\mathcal{R}})$ can be written as a function of the landmarks as follows

$$V_q(\widetilde{\mathcal{R}}) = \frac{1}{2}\operatorname{trace}\left((L - L_q^\star)(\mathbf{I}_n - \mathbf{a}\mathbf{1}^\top)D_a(\mathbf{I}_n - \mathbf{1}\mathbf{a}^\top)(L - L_q^\star)^\top\right), \tag{31}$$

where $L_q^\star$ is given by

$$L_q^\star := \mathcal{R}_d^\top \exp(-k_q P_M(L) S(\mathbf{u}_q))X - \mathbf{p}_d\mathbf{1}^\top.$$

Again, since the function $V_q(\widetilde{\mathcal{R}})$ can be written as a function of the landmarks, we use the notation $V_q(L)$ in the sequel. Naturally, it is straightforward to verify that $\rho(\widetilde{\mathcal{R}}) := \min_{q\in Q} \mathcal{V}_q(\widetilde{\mathcal{R}})$ can be written as a function of the landmarks as well, thus we use the notation $\rho(L)$ when referring to this function herein.

Prepared using rncauth.cls
DOI: 10.1002/rnc

Using the previous remarks, we define the closed-loop hybrid system

$$\textbf{State: } x = (\widetilde{\mathbf{p}}, \widetilde{\mathcal{R}}, \widetilde{\mathbf{v}}, \widetilde{\boldsymbol{\omega}}, q, \mathbf{p}_d, \mathcal{R}_d, \mathbf{v}_d, \boldsymbol{\omega}_d) \tag{32a}$$

$$\textbf{Flow Map: } F(x) = \begin{pmatrix} \widetilde{\mathbf{v}} - S(\widetilde{\boldsymbol{\omega}} + \boldsymbol{\omega}_d)\widetilde{\mathbf{p}} + S(\mathbf{p}_d)\widetilde{\boldsymbol{\omega}} \\ -S(\mathcal{R}_d\widetilde{\boldsymbol{\omega}})\widetilde{\mathcal{R}} \\ \mathbf{u}_{\mathbf{v}}(L, \dot{L}, \boldsymbol{\omega}, x_d) \\ \mathbf{u}_{\boldsymbol{\omega}}(L, \dot{L}, \boldsymbol{\omega}, x_d) \\ 0 \\ f_d(\mathbf{p}_d, \mathcal{R}_d, \mathbf{v}_d, \boldsymbol{\omega}_d) \end{pmatrix}, \forall x \in C \tag{32b}$$

$$\textbf{Flow Set: } C = \{x \in SE(3) \times \mathbb{R}^6 \times Q \times SE(3) \times \mathbb{R}^6 : V_q(L) - \rho(L) \leq \delta\} \tag{32c}$$

Jump Map:

$$G(x) = \{(\widetilde{\mathbf{p}}, \widetilde{\mathcal{R}}, \widetilde{\mathbf{v}}, \widetilde{\boldsymbol{\omega}})\} \times \{q' \in Q : V_{q'}(L) = \rho(L)\} \times \{(\mathbf{p}_d, \mathcal{R}_d, \mathbf{v}_d, \boldsymbol{\omega}_d)\}, \forall x \in D \tag{32d}$$

$$\textbf{Jump Set: } D = \{x \in SE(3) \times \mathbb{R}^6 \times Q \times SE(3) \times \mathbb{R}^6 : V_q(L) - \rho(L) \geq \delta\}, \tag{32e}$$

where $\mathbf{u}_{\mathbf{v}}(L, \dot{L}, \boldsymbol{\omega}, x_d)$ and $\mathbf{u}_{\boldsymbol{\omega}}(L, \dot{L}, \boldsymbol{\omega}, x_d)$ are given by

$$\mathbf{u}_{\mathbf{v}}(L, \dot{L}, \boldsymbol{\omega}, x_d) = k_{\mathbf{v}}\left((\dot{L} + S(\boldsymbol{\omega})L)\mathbf{a} + \mathbf{v}_d\right) - k_{\mathbf{p}}(L_d - L)\mathbf{a},$$

$$\mathbf{u}_{\boldsymbol{\omega}}(L, \dot{L}, \boldsymbol{\omega}, x_d) = -k_{\boldsymbol{\omega}}(\boldsymbol{\omega} - \boldsymbol{\omega}_d) + k_{\mathbf{p}}S(\mathbf{p}_d)(\boldsymbol{\omega} - \boldsymbol{\omega}_d)$$

$$- k_{\mathcal{R}}(\mathbf{I}_3 + k_q\varphi(L(\mathbf{I}_n - \mathbf{a}\mathbf{1}^\top)D_a(\mathbf{I}_n - \mathbf{1}\mathbf{a}^\top)L_d^\top)\mathbf{u}_q^\top\mathcal{R}_d)\varphi(L_q^\star(\mathbf{I}_n - \mathbf{a}\mathbf{1}^\top)D_a(\mathbf{I}_n - \mathbf{1}\mathbf{a}^\top)L).$$

The global asymptotic stability of the set $\mathcal{A}_{\mathcal{H}}$ for the hybrid system (32) follows from the simple observation that (33) is equivalent to (14), as proved next.

Theorem 6
Let Assumptions 1, 2 and 3 be satisfied. Then, there exists $k > 0$ satisfying (25) and $\delta > 0$, such that there exists a family of synergistic potential functions on $SO(3)$ with gap exceeding δ. Moreover, for any $k_{\mathcal{R}}, k_{\boldsymbol{\omega}}, k_{\mathbf{p}}, k_{\mathbf{v}} > 0$, the set (16) is globally asymptotically stable for the hybrid system (32).

Proof
It follows from Assumptions 2 and 3 that there exists $\mathbf{a} \in \mathbb{R}^n$ such that $M := XD_aX^\top$ is positive definite with distinct eigenvalues. Consequently, it follows from Theorem 5 that (23) forms a family of synergistic potential functions on $SO(3)$ with gap exceeding δ, for some $\delta > 0$ and for any k satisfying (25).

Since (23) can be written as a function of the landmarks as shown in (31), we can claim that the jump set, jump map and flow set of (15) and (32) are the same.

Next, we prove that (33) is equivalent to (14). The position error $\widetilde{\mathbf{p}}$ can be computed from L and L_d using the relation

$$\widetilde{\mathbf{p}} = (L_d - L)\mathbf{a},$$

for some $\mathbf{a} \in \mathbb{R}^n$ satisfying Assumption 3. The linear velocity $\mathbf{v}$ can be computed from L, $\dot{L}$ and $\boldsymbol{\omega}$ using the relation

$$\mathbf{v} = -(\dot{L} + S(\boldsymbol{\omega})L)\mathbf{a}. \tag{34}$$

At this point, the only term of (21) that remains to be rewritten as a function of the sensor measurements is $\mathcal{R}_d^\top\widetilde{\mathcal{R}}\varphi(\widetilde{\mathcal{R}}^\top\nabla V_q(\widetilde{\mathcal{R}})) = \mathcal{R}^\top\varphi(\widetilde{\mathcal{R}}^\top\nabla V_q(\widetilde{\mathcal{R}}))$ and this is achieved by the following set of computations. Applying (29) to $\mathcal{R}^\top\varphi(\widetilde{\mathcal{R}}^\top\nabla V_q(\widetilde{\mathcal{R}}))$ we obtain

$$\mathcal{R}^\top\varphi(\widetilde{\mathcal{R}}^\top\nabla V_q(\widetilde{\mathcal{R}})) = -\mathcal{R}^\top\Theta(\widetilde{\mathcal{R}}, q)^\top\varphi(\mathcal{T}_q(\widetilde{\mathcal{R}})^\top M), \tag{35}$$

Replacing (30) and (24) into (35) yields

$$\mathcal{R}^\top\varphi(\widetilde{\mathcal{R}}^\top\nabla V_q(\widetilde{\mathcal{R}})) = -\mathcal{R}^\top(\mathbf{I}_3 + k_q\widetilde{\mathcal{R}}^\top\mathbf{u}_q\varphi(\widetilde{\mathcal{R}}M)^\top\widetilde{\mathcal{R}})^\top\varphi(\widetilde{\mathcal{R}}^\top\exp(-k_qP_M(\widetilde{\mathcal{R}})S(\mathbf{u}_q)))M). \tag{36}$$

Prepared using rncauth.cls
DOI: 10.1002/rnc

Replacing $\Phi := \exp(-k_q P_M(\widetilde{\mathcal{R}})S(\mathbf{u}_q)))$ and $M := XD_aX^\top$ into (36) yields

$$\mathcal{R}^\top\varphi(\widetilde{\mathcal{R}}^\top\nabla V_q(\widetilde{\mathcal{R}})) = -\mathcal{R}^\top(\mathbf{I}_3 + k_q\mathcal{R}\mathcal{R}_d^\top\mathbf{u}_q\varphi(\mathcal{R}_d\mathcal{R}^\top XD_aX^\top)^\top\mathcal{R}_d\mathcal{R}^\top)^\top\varphi(\mathcal{R}\mathcal{R}_d^\top\Phi^\top XD_aX^\top).$$

Using the distributive property of matrix multiplication and using $\mathcal{R}\varphi(A) = \varphi(\mathcal{R}A\mathcal{R}^\top)$ we obtain the following expression after some manipulations

$$\mathcal{R}^\top\varphi(\widetilde{\mathcal{R}}^\top\nabla V_q(\widetilde{\mathcal{R}})) = -(\mathbf{I}_3 + k_q\varphi(\mathcal{R}^\top XD_aX^\top\mathcal{R}_d)\mathbf{u}_q^\top\mathcal{R}_d)\varphi(\mathcal{R}_d^\top\Phi^\top XD_aX^\top\mathcal{R}).$$

Finally, using the relations $\widetilde{\boldsymbol{\omega}} = \boldsymbol{\omega} - \boldsymbol{\omega}_d$, (11a), $\mathcal{R}^\top X = L(\mathbf{I}_n - \mathbf{a}\mathbf{1}^\top)$, $\mathcal{R}_d^\top X = L_d(\mathbf{I}_n - \mathbf{a}\mathbf{1}^\top)$ and $\mathcal{R}_d^\top\Phi^\top X = L_q^\star(\mathbf{I}_n - \mathbf{a}\mathbf{1}^\top)$ (which follow from Assumption 2), we obtain (33) from (14). □

From Theorem 6 and (34), we conclude that the control law (12) can be written as a function of the reference trajectory and of the sensor measurements L, $\dot{L}$ and $\boldsymbol{\omega}$, denoted by $\kappa(L, \dot{L}, \boldsymbol{\omega}, x_d)$,

$$\begin{aligned}\mathbf{f} &= m(\dot{\mathbf{v}}_d - S(\boldsymbol{\omega})(\dot{L} + S(\boldsymbol{\omega})L)\mathbf{a} + k_{\mathbf{v}}\left((\dot{L} + S(\boldsymbol{\omega})L)\mathbf{a} + \mathbf{v}_d\right) - k_{\mathbf{p}}(L_d - L)\mathbf{a},\\ \boldsymbol{\tau} &= -S(\mathbf{J}\boldsymbol{\omega})\boldsymbol{\omega} + \mathbf{J}(\dot{\boldsymbol{\omega}}_d - k_{\boldsymbol{\omega}}(\boldsymbol{\omega} - \boldsymbol{\omega}_d) + S(\mathbf{p}_d)(L_d - L)\mathbf{a}\\ &\quad - k_{\mathcal{R}}(\mathbf{I}_3 + k_q\varphi(L(\mathbf{I}_n - \mathbf{a}\mathbf{1}^\top)D_a(\mathbf{I}_n - \mathbf{1}\mathbf{a}^\top)L_d^\top)\mathbf{u}_q^\top\mathcal{R}_d)\varphi(L_q^\star(\mathbf{I}_n - \mathbf{a}\mathbf{1}^\top)D_a(\mathbf{I}_n - \mathbf{1}\mathbf{a}^\top)L)).\end{aligned} \tag{37}$$

Moreover, since $\mathrm{proj}_{SE(3)\times\mathbb{R}^6}(\mathcal{A}_\mathcal{H}) = \{0\}\times\{\mathbf{I}_3\}\times\{0\}\times\{0\} = \mathcal{A}$, where the operator $\mathrm{proj}_X(X\times Y) = X$ denotes the canonical projection operator, the stability of the set $\mathcal{A}$ does not depend on the initial condition of the logic variable. In the following section we illustrate the behaviour of the closed-loop hybrid system in a simulation environment.

5. SIMULATION RESULTS

In this section, we present some simulation results for the hybrid controller proposed in Section 4. We present two scenarios. In the first scenario, the initial attitude is a critical point of $P_M(\widetilde{\mathcal{R}})$. In the second scenario, the initial attitude is a critical point of V_q. In both situations, the starting position is displaced with respect to the desired position, thus the initial position error $\widetilde{\mathbf{p}}(0)$ is different than 0.

For this set of simulations, we designed a reference trajectory which verifies the dynamics of a vectored-thrust vehicle (e.g., quadrotor), given by

$$m\ddot{\mathbf{p}}_I = \mathcal{R}\mathbf{e}_3 T - mg\mathbf{e}_3.$$

where $m = 1$ kg is the mass of the vehicle, $g = 9.81$ m/s^2 is the acceleration of gravity, $\mathbf{p}_I \in \mathbb{R}^3$ denotes the position of the vehicle in the frame $\{I\}$, $\mathbf{e}_3 = [0\ 0\ 1]^\top$ and $T \in \mathbb{R}$ denotes the thrust of the vehicle. In particular, we choose

$$f_d(x_d) := \begin{pmatrix} \mathbf{v}_d - S(\boldsymbol{\omega}_d)\mathbf{p}_d \\ -\mathbf{p}_d - S(\boldsymbol{\omega}_d)\mathbf{v}_d \\ \mathcal{R}_d S(\boldsymbol{\omega}_d) \\ S(\mathbf{e}_3)\mathcal{R}_d^\top\frac{d^2}{dt^2}\left(\frac{-\mathcal{R}_d\mathbf{p}_d + ge_3}{|-\mathcal{R}_d\mathbf{p}_d + ge_3|}\right)\end{pmatrix}, \tag{38}$$

and $x_d(0,0) = (p_d, v_d, \mathcal{R}_d, \omega_d)(0,0)$ with

$$p_d(0,0) \approx \begin{bmatrix} 0.0913 \\ -0.9958 \\ 0 \end{bmatrix}, \quad \mathcal{R}_d(0,0) \approx \begin{bmatrix} 0.0913 & -0.9958 & 0 \\ 0.9916 & 0.0908 & -0.1014 \\ 0.0913 & 0.0093 & 0.9948 \end{bmatrix},$$

$$v_d(0,0) \approx \begin{bmatrix} 0.9916 \\ 0.0908 \\ -0.1014 \end{bmatrix}, \quad \omega_d(0,0) \approx \begin{bmatrix} 0.1010 \\ 0.0093 \\ 0 \end{bmatrix},$$

Prepared using rncauth.cls
DOI: 10.1002/rnc

which is such that $\mathbf{p}_I(t,j) = [\cos(t)\ \sin(t)\ 0]^\top$ for all $(t,j) \in \operatorname{dom} x$.* The chosen landmarks for these simulations are given in (13) and depicted in Figure 1. It is possible to verify that, for these parameters and $k_1 = 0.1$, $k_2 = -0.1$ and $\mathbf{u}_1 = \mathbf{u}_2 = \mathbf{z}/|\mathbf{z}|$ with $\mathbf{z} = \begin{bmatrix}0 & 1 & 1\end{bmatrix}^\top$, the functions $V_1(\widetilde{\mathcal{R}}) = P_M(\mathcal{T}_1(\widetilde{\mathcal{R}}))$ and $V_2(\widetilde{\mathcal{R}}) = P_M(\mathcal{T}_2(\widetilde{\mathcal{R}}))$ are synergistic with gap exceeding $\delta = 0.0017$. The controller parameters $k_{\mathbf{p}}$, $k_{\mathcal{R}}$, $k_{\mathbf{p}}$, and $k_{\boldsymbol{\omega}}$ should be tuned to the specific application at hand. In general, increasing these parameters leads to faster response times and increased disturbance rejection, at the cost of higher actuation authority. In the simulations we chose $k_{\mathbf{p}} = k_{\mathcal{R}} = k_{\mathbf{p}} = k_{\boldsymbol{\omega}} = 1$.

In the following simulations, we also compare the performance of the hybrid controller with the standard continuous feedback law that is obtained by setting $k_q = 0$ in (37), which is

$$\begin{aligned}
\mathbf{f} &= m(\dot{\mathbf{v}}_d - S(\boldsymbol{\omega})(\dot{L} + S(\boldsymbol{\omega})L)\mathbf{a} + k_{\mathbf{v}}\left((\dot{L} + S(\boldsymbol{\omega})L)\mathbf{a} + \mathbf{v}_d\right) - k_{\mathbf{p}}(L_d - L)\mathbf{a},\\
\boldsymbol{\tau} &= -S(\mathbf{J}\boldsymbol{\omega})\boldsymbol{\omega} + \mathbf{J}\dot{\boldsymbol{\omega}}_d - k_{\boldsymbol{\omega}}(\boldsymbol{\omega} - \boldsymbol{\omega}_d) + S(\mathbf{p}_d)(\boldsymbol{\omega} - \boldsymbol{\omega}_d)\\
&\quad - k_{\mathcal{R}}\varphi(L_d(\mathbf{I}_n - \mathbf{a}\mathbf{1}^\top)D_a(\mathbf{I}_n - \mathbf{1}\mathbf{a}^\top)L).
\end{aligned}$$

The nature of the hybrid and the continuous control law is very different. The continuous feedback law renders $\mathcal{A}$ *almost globally asymptotically stable*, i.e., it is unable to steer the vehicle towards the desired attitude if it starts in an unwanted critical point and, even if it does not, the influence of arbitrarily small noise may degrade the convergence rate to the desired set-point or, in a worst-case scenario, completely prevent its stabilization. In order to illustrate this phenomenon, let us consider a simplified scenario where the attitude of the rigid body is given by

$$\mathcal{R}(\theta, \mathbf{z}) = \begin{bmatrix}\cos\theta & -\sin\theta & 0\\ \sin\theta & \cos\theta & 0\\ 0 & 0 & 1\end{bmatrix}, \tag{40}$$

with $\theta \in \mathbb{R}$ and $\mathbf{z} = \begin{bmatrix}0 & 0 & 1\end{bmatrix}^\top$. Let $M_1 = M_2 = \mathbf{I}_3$, $\mathbf{u}_1 = \mathbf{u}_2 = \mathbf{z}$ and $k_1 = -k_2 = k > 0$. Under these conditions, one may check that the critical points of each Lyapunov function $V_q(\widetilde{\mathcal{R}}) = P_{M_q}(\mathcal{T}_q(\widetilde{\mathcal{R}}))$ are at $\theta = 0$ and at the point $\theta_0 \neq 0$ which is solution to the algebraic equation

$$\sin(2k(1 - \cos\theta_0) + \theta_0) = 0.$$

Two synergistic Lyapunov functions have their critical point apart from each other, enabling hysteretic switching between the controllers, as shown in Figure 2. Notice that while this choice of parameters provides a family of synergistic potential functions in the simplified case of $SO(2)$ (40), it does not work if $\widetilde{\mathcal{R}} \in SO(3)$ because the criteria (26) are not met.

For the first simulation, we selected the following initial condition

$$\begin{aligned}
&\mathbf{p}(0,0) = \begin{bmatrix}1\\0\\0\end{bmatrix}, \quad \mathcal{R}(0,0) \approx \begin{bmatrix}-0.0913 & 0.9958 & -0.0000\\ 0.9916 & 0.0908 & -0.1014\\ -0.0913 & -0.0093 & -0.9948\end{bmatrix},\\
&\mathbf{v}(0,0) = 0 \qquad \boldsymbol{\omega}(0,0) = 0,
\end{aligned}$$

which is such that $\widetilde{\mathcal{R}}(0,0)$ is in a neighbourhood of Crit P_M and the initial position is offset from the desired one.

Figure 3 depicts the evolution of the distance between $\mathcal{R}(t)$ and $\mathcal{R}_d \in SO(3)$ (measured in terms of trace$(\mathbf{I}_3 - \widetilde{\mathcal{R}})$) and the norm of the position, linear velocity and angular velocity

*Notice that the term

$$\frac{d^2}{dt^2}\left(\frac{-\mathcal{R}_d\mathbf{p}_d + ge_3}{|-\mathcal{R}_d\mathbf{p}_d + ge_3|}\right)$$

in (38) is a function of the reference trajectory x_d.

Prepared using rncauth.cls
DOI: 10.1002/rnc

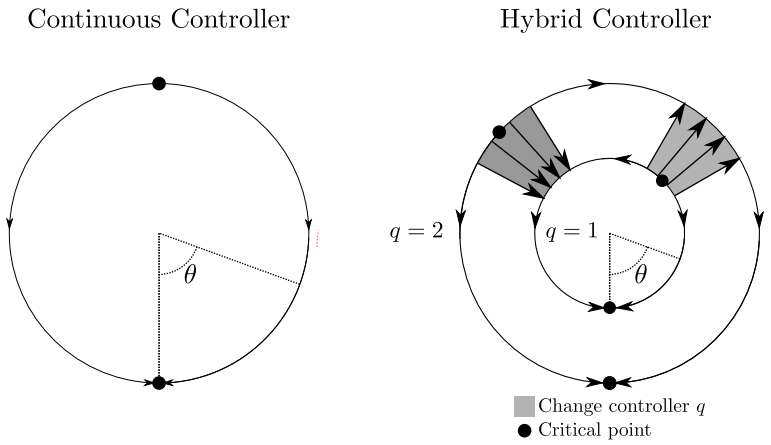

Figure 2. Comparison between the simplified hybrid and continuous closed-loop systems. The existence of hysteretic switching in the hybrid system increases the robustness to measurement noise.

errors, denoted by $|\widetilde{\mathbf{p}}(t)|$, $|\widetilde{\mathbf{v}}(t)|$ and $|\widetilde{\boldsymbol{\omega}}(t)|$, respectively. In this simulation, we consider an additive disturbance signal to the torque, denoted by $d(\widetilde{\mathcal{R}}, q)$, and given by

$$d(\widetilde{\mathcal{R}}, q) = (1+\epsilon)\Theta(\widetilde{\mathcal{R}}, q)^{\top}\varphi(\mathcal{T}_q(\widetilde{\mathcal{R}})M), \tag{41}$$

where $\epsilon > 0$. Notice that this disturbance is 0 if and only if $\widetilde{\mathcal{R}} \in \text{Crit } V_q$ and since it overcomes the negative attitude feedback, the attitude error of the continuous system converges to an unwanted critical point on the $SO(3)$ manifold while the disturbance signal converges to 0, as suggested by Figure 4. Since the unwanted critical points Crit $V_q \backslash \mathbf{I}_3$ lie in the jump set D of the hybrid system, the hybrid controller switches and is able to drive the rotation error $\widetilde{\mathcal{R}}$ to the identity matrix. Nevertheless, both controllers are able to track the position, tangential velocity, and angular velocity components of the reference trajectory x_d. However, it should be clear from the analysis of Figure 4 that the continuous controller tracks the desired position trajectory with an attitude error of 180°.

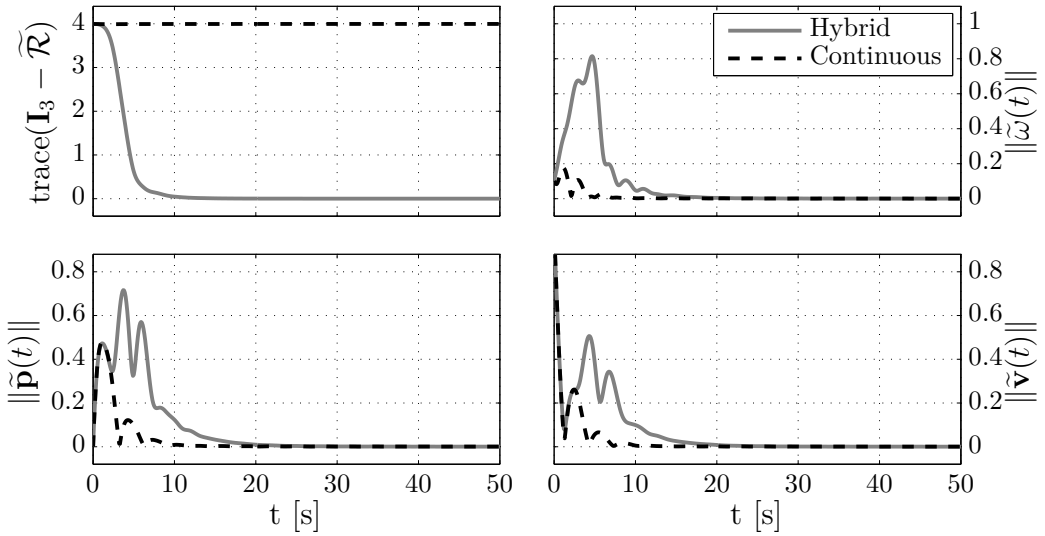

Figure 3. Simulation results for an initial condition close to a critical point of P_M under the influence of the disturbance (41)

DOI: 10.1002/rnc

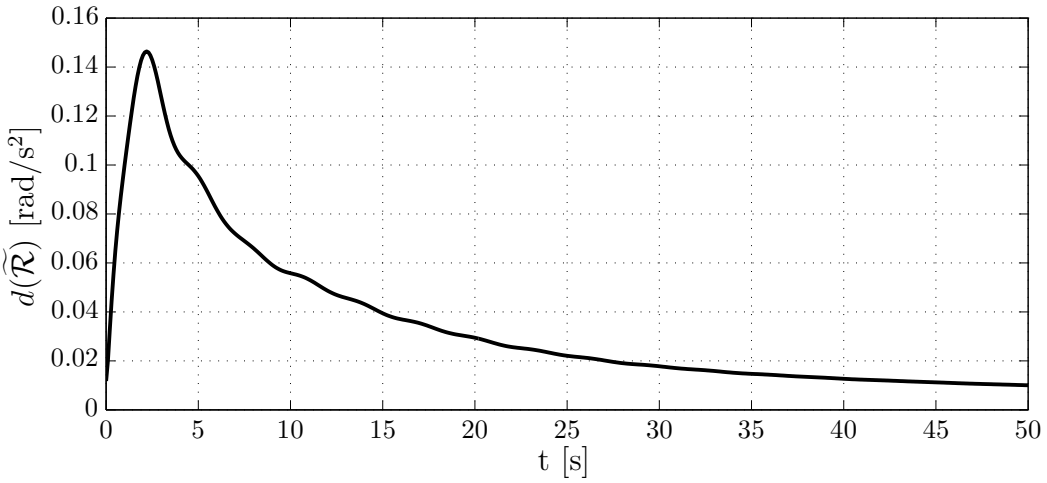

Figure 4. Disturbance signal (41) used in the first simulation.

For the second simulation, we changed the initial rotation matrix to

$$\mathcal{R}(0,0) \approx \begin{bmatrix} 0.0979 & 0.9695 & -0.2256 \\ 0.9909 & -0.1159 & -0.0777 \\ -0.0920 & -0.2160 & -0.9711 \end{bmatrix},$$

so as to place $\widetilde{\mathcal{R}}(0,0)$ near a critical point of $P_M(\mathcal{T}_1(\mathcal{R}_e))$. Since $q(0,0) = 1$, the initial condition lies in the jump set, immediately changing the mode of the controller to $q = 2$. It can be seen in Figure 5 that the performance of the two controllers are similar in this situation. This is so because the family of synergistic potential functions used in this application is very close to the original modified trace function (that is, before using the angular warping technique), as reflected in the small synergy gap δ. The synergy gap may be increased by appropriate tuning of the parameters k_1 and k_2, but it is ultimately constrained by the geometry of the landmarks, since it depends on the eigenvalues of $XD_{\mathbf{a}}X^\top$.

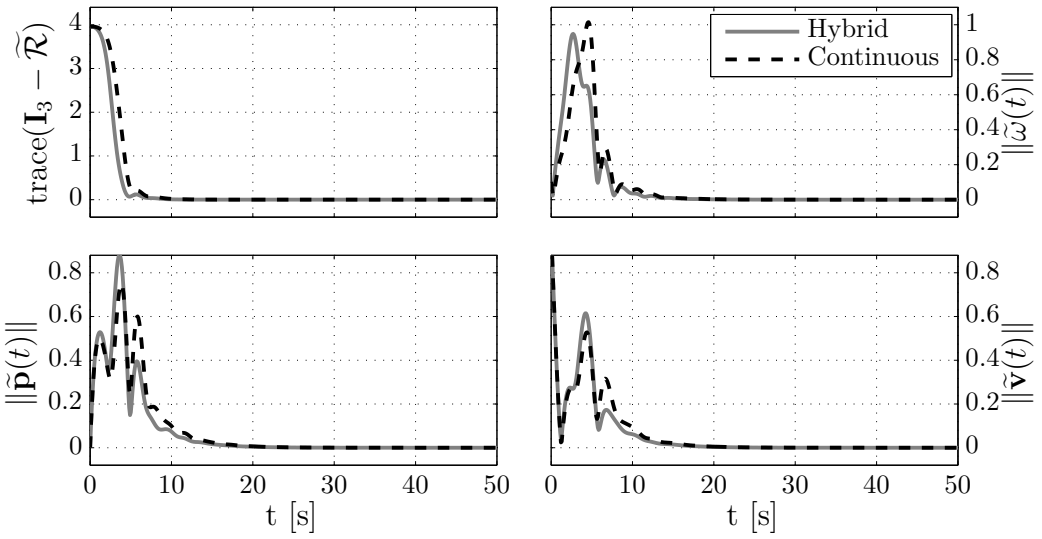

Figure 5. Simulation results for an initial condition close to a critical point of V_q.

DOI: 10.1002/rnc

6. CONCLUSIONS

In this work we have presented a control law which enables the global asymptotic stabilization of a fully actuated rigid body to a desired trajectory in $SE(3) \times \mathbb{R}^6$, using the measurements from the angular velocity, the locations of given landmarks and their rate of change. We have employed recent developments on synergistic Lyapunov functions and proved that, under mild assumptions on the geometry of the landmarks, the problem is solved by the proposed control law. We also presented simulation results which illustrate the advantages of the proposed control law over standard continuous feedback strategies.

References

1. Mortensen RE. A globally stable linear attitude regulator. *International Journal of Control* 1968; **8**(3):297–302, doi:10.1080/00207176808905679.
2. Koditschek DE. The application of total energy as a Lyapunov function for mechanical control systems. *Contemporary Mathematics, vol. 97, American Mathematical Society, 1989* 1989; .
3. Wen JY, Kreutz-Delgado K. The attitude control problem. *IEEE Transactions on Automatic Control* oct 1991; **36**(10):1148 –1162, doi:10.1109/9.90228.
4. Bhat SP, Bernstein DS. A topological obstruction to continuous global stabilization of rotational motion and the unwinding phenomenon. *Systems & Control Letters* 2000; **39**(1):63 – 70, doi:10.1016/S0167-6911(99)00090-0.
5. Nicolaescu L. *An Invitation to Morse Theory*. Universitext - Springer-Verlag, Springer, 2011. URL `http://books.google.pt/books?id=nCgvt2MY4QAC`.
6. Shuster MD. A survey of attitude representations. *The Journal of Astronautical Sciences* 1993; **41**(4):439–517.
7. Meyer G. Design and global analysis of spacecraft attitude control systems. *Technical Report*, NASA, Ames Research Center 1971.
8. Wisniewski R, Kulczycki P. Rotational motion control of a spacecraft. *IEEE Transactions on Automatic Control* april 2003; **48**(4):643 – 646, doi:10.1109/TAC.2003.809781.
9. Chaturvedi N, McClamroch N. Almost global attitude stabilization of an orbiting satellite including gravity gradient and control saturation effects. *American Control Conference*, 2006; 1748–1753.
10. Kristiansen R, Nicklasson P, Gravdahl J. Satellite attitude control by quaternion-based backstepping. *IEEE Transactions on Control Systems Technology* Jan 2009; **17**(1):227 –232, doi:10.1109/TCST.2008.924576.
11. Hua M, Hamel T, Morin P, Samson C. A control approach for thrust-propelled underactuated vehicles and its application to VTOL drones. *IEEE Transactions on Automatic Control* 2009; **54**(8):1837 –1853.
12. Fjellstad OE, Fossen T. Quaternion feedback regulation of underwater vehicles. *Proceedings of the Third IEEE Conference on Control Applications*, 1994; 857 –862 vol.2, doi:10.1109/CCA.1994.381209.
13. Bauchau OA, Trainelli L. The vectorial parametrization of rotation. *Nonlinear Dynamics* 2003; **32(1)**:49–71.
14. Stuelpnagel J. Ont the parametrization of the three-dimensional rotation group. *SIAM Review* 1964; **6**(4).
15. Chaturvedi N, Sanyal A, McClamroch N. Rigid-body attitude control. *IEEE Control Systems Magazine* june 2011; **31**(3):30 –51, doi:10.1109/MCS.2011.940459.
16. Joshi S, Kelkar A, Wen JY. Robust attitude stabilization of spacecraft using nonlinear quaternion feedback. *IEEE Transactions on Automatic Control* oct 1995; **40**(10):1800 –1803, doi:10.1109/9.467669.
17. Tayebi A, McGilvray S. Attitude stabilization of a VTOL quadrotor aircraft. *IEEE Transactions on Control Systems Technology* may 2006; **14**(3):562 – 571, doi:10.1109/TCST.2006.872519.
18. CG Mayhew, RG Sanfelice, AR Teel. On quaternion-based attitude control and the unwinding phenomenon. *American Control Conference (ACC)*, 2011; 299 –304.
19. Wertz JR. *Spacecraft Attitude Determination and Control*. Kluwer Academic Publishers, 1978.
20. Markley FL. Attitude determination using observations and the singular value decomposition. *The Journal of Astronautical Sciences* 1988; .
21. Kristiansen R, Nicklasson P, Gravdahl J. Satellite attitude control by quaternion-based backstepping. *Control Systems Technology, IEEE Transactions on* jan 2009; **17**(1):227 –232, doi:10.1109/TCST.2008.924576.
22. Li S, Ding S, Li Q. Global set stabilization of the spacecraft attitude control problem based on quaternion. *International Journal of Robust and Nonlinear Control* 2010; **20**(1):84–105, doi:10.1002/rnc.1423.
23. Mayhew CG, Teel AR. On the topological structure of attraction basins for differential inclusions. *Systems & Control Letters* 2011; **60**(12):1045 – 1050, doi:10.1016/j.sysconle.2011.07.012.
24. RG Sanfelice, MJ Messina, Emre Tuna S, AR Teel. Robust hybrid controllers for continuous-time systems with applications to obstacle avoidance and regulation to disconnected set of points. *American Control Conference*, 2006; 3352–3357, doi:10.1109/ACC.2006.1657236.
25. Goebel R, Sanfelice RG, Teel AR. Hybrid dynamical systems. *IEEE Control Systems Magazine* April 2009; **29**(2):28 –93, doi:10.1109/MCS.2008.931718.

26. Goebel R, Sanfelice RG, Teel AR. *Hybrid Dynamical Systems: Modeling, Stability and Robustness*. Princeton University Press, 2012.
27. CG Mayhew, RG Sanfelice, AR Teel. Robust global asymptotic attitude stabilization of a rigid body by quaternion-based hybrid feedback. *Proceedings of the 48th IEEE Conference on Decision and Control, held jointly with the 28th Chinese Control Conference*, 2009; 2522 –2527, doi: 10.1109/CDC.2009.5400431.
28. CG Mayhew, AR Teel. Hybrid control of rigid-body attitude with synergistic potential functions. *American Control Conference (ACC)*, 2011; 287 –292.
29. Fjellstad OE, Fossen T. Singularity-free tracking of unmanned underwater vehicles in 6 dof. *Proceedings of the 33rd IEEE Conference on Decision and Control*, vol. 2, 1994; 1128 –1133, doi: 10.1109/CDC.1994.411068.
30. Bullo F, Murray RM. Tracking for fully actuated mechanical systems: a geometric framework. *Automatica* 1999; **35**(1):17 – 34, doi:10.1016/S0005-1098(98)00119-8.
31. Frazzoli E, Dahleh M, Feron E. Trajectory tracking control design for autonomous helicopters using a backstepping algorithm. *Proceedings of the American Control Conference*, vol. 6, 2000; 4102 –4107, doi:10.1109/ACC.2000.876993.
32. Aguiar A, Hespanha J. Position tracking of underactuated vehicles. *Proceedings of the American Control Conference*, vol. 3, 2003; 1988 – 1993 vol.3, doi:10.1109/ACC.2003.1243366.
33. CG Mayhew, RG Sanfelice, AR Teel. Robust global asymptotic stabilization of a 6-dof rigid body by quaternion-based hybrid feedback. *Proceedings of the 48th IEEE Conference on Decision and Control, held jointly with the 28th Chinese Control Conference*, 2009; 1094 –1099, doi: 10.1109/CDC.2009.5400338.
34. Cunha R, Silvestre C, Hespanha JP. Output-feedback control for stabilization on SE(3). *Systems & Control Letters* 2008; **57**(12):1013–1022.
35. Cabecinhas D, Cunha R, Silvestre C. Almost global stabilization of fully-actuated rigid bodies. *Systems & Control Letters* 2009; **58**(9):639 – 645, doi:10.1016/j.sysconle.2009.04.007.
36. Khosravian A, Namvar M. Rigid body attitude control using a single vector measurement and gyro. *IEEE Transactions on Automatic Control* may 2012; **57**(5):1273 –1279, doi:10.1109/TAC.2011.2174663.
37. P Casau, RG Sanfelice, R Cunha, C Silvestre. A landmark-based controller for global asymptotic stabilization on se(3). *IEEE Conference on Decision and Control*, 2012.
38. Boyd S, Vandenberghe L. *Convex Optimization*. Cambridge University Press: New York, NY, USA, 2004.
39. Lee J. *Introduction to Smooth Manifolds*. Graduate Texts in Mathematics, Springer, 2003. URL `http://books.google.com/books?id=eqfgZtjQceYC`.
40. Hall B. *Lie Groups, Lie Algebras, and Representations: An Elementary Introduction*. Graduate Texts in Mathematics, Springer, 2003. URL `http://books.google.pt/books?id=m1VQi8HmEwcC`.
41. Mayhew CG, Teel AR. Synergistic potential functions for hybrid control of rigid-body attitude. *American Control Conference (ACC)*, 2011; 875 –880.
42. Betty MF. *Principles of Engineering Mechanics*, vol. 1. Plenum Press, 1986.
43. Grip H, Fossen T, Johansen T, Saberi A. Attitude estimation using biased gyro and vector measurements with time-varying reference vectors. *IEEE Transactions on Automatic Control* 2012; **57**(5):1332–1338, doi:10.1109/TAC.2011.2173415.
44. Tenenbaum RA. *Fundamentals of Applied Dynamics*. Springer-Verlag New York, Inc., 2004.
45. Lee J. *Introduction to topological manifolds*. Graduate texts in mathematics, SPRINGER VERLAG GMBH, 2000. URL `http://books.google.com/books?id=wyuzE2lSPAgC`.
46. Lütkepohl H. *Handbook of Matrices*. John Wiley & Sons, 1996.

A. PROOF OF THEOREM 5

From (23), we have that $V_q(\mathcal{R}) = P_{M_q}(\mathcal{T}_q(\mathcal{R}))$. Since (22) is real valued and continuously differentiable in $SO(3)$ and, by assumption, $k_q \in \mathbb{R}$ and $\mathbf{u}_q \in \mathbb{S}^2$, we know from [41, Theorem 8] that (24) is a diffeomorphism in $SO(3)$, provided that (25) holds. From [41, Corollary 9], we have that $V_q(\mathcal{R})$ is a potential function on $SO(3)$ and, consequently, $\mathscr{V} := \{V_1(\mathcal{R}), V_2(\mathcal{R})\}$ is a family of potential functions on $SO(3)$.

Prepared using rncauth.cls
DOI: 10.1002/rnc

Using (5), (23), $M_1 = M_2 = M$, $\mathbf{u}_1 = \mathbf{u}_2 = \mathbf{u}$ and the definition of $\mathscr{V}$, we are able to obtain the following expression for the synergy gap $\mu(\mathscr{V})$:

$$\begin{aligned}\mu(\mathscr{V}) = & \min_{\substack{q\in Q\\ \mathcal{R}\in \text{Crit } V_q\setminus\{\mathbf{I}_3\}}} \max\{0, \text{trace}((\mathbf{I}_3 - e^{k_q P_M(\mathcal{R})S(\mathbf{u})}\mathcal{R})M) \\ & - \text{trace}((\mathbf{I}_3 - e^{-k_q P_M(\mathcal{R})S(\mathbf{u})}\mathcal{R})M)\} \\ = & \min_{\substack{q\in Q\\ \mathcal{R}\in \text{Crit } V_q\setminus\{\mathbf{I}_3\}}} \max\{0, \text{trace}((e^{-2k_q P_M(\mathcal{R})S(\mathbf{u})} - \mathbf{I}_3)e^{k_q P_M(\mathcal{R})S(\mathbf{u})}\mathcal{R}M)\} \\ = & \max\left\{0, \min_{\substack{q\in Q\\ \mathcal{R}\in \text{Crit } V_q\setminus\{\mathbf{I}_3\}}} \text{trace}((e^{-2k_q P_M(\mathcal{R})S(\mathbf{u})} - \mathbf{I}_3)e^{k_q P_M(\mathcal{R})S(\mathbf{u})}\mathcal{R}M)\right\}.\end{aligned} \tag{42}$$

From [41, Theorem 6] and (23), we have that Crit $V_q = \mathcal{T}_q^{-1}(\text{Crit } P_M)$ or, equivalently, $\mathcal{T}_q(\text{Crit } V_q) = \text{Crit } P_M$. We also know from [2, Lemma 4.1] that

$$\text{Crit } P_M = \{\mathbf{I}_3\} \cup \left\{ \bigcup_{i\in\{1,2,3\}} \{\mathcal{R}(\pi, \mathbf{v}_i)\} \right\},$$

where $\mathbf{v}_i \in \mathbb{S}^2$ is a normalized eigenvector of $M \in \mathbb{R}^{3\times 3}$. Using the previous two facts, we have that

$$e^{k_q P_M(\mathcal{R}_{q_i})S(\mathbf{u})}\mathcal{R}_{q_i} = \mathcal{R}(\pi, \mathbf{v}_i) \quad \forall i \in \{1,2,3\}, \tag{43}$$

where $\mathcal{R}_{q_i} \in SO(3)$ denotes the i-th element of Crit $V_q\setminus\{\mathbf{I}_3\} \subset SO(3)$. From [46, Section 9.13.3], we have that the matrix M can be expressed as a function of its eigenvalues and unitary-norm eigenvectors as follows

$$M = \sum_{j=1}^{3} \lambda_j \mathbf{v}_j \mathbf{v}_j^\top,$$

and, using (4) and the relation $S(\mathbf{u})^2 = \mathbf{u}\mathbf{u}^\top - \mathbf{u}^\top\mathbf{u}\,\mathbf{I}_3$, we have that

$$\begin{aligned} e^{kP_M(\mathcal{R}_{q_i})S(\mathbf{u})}\mathcal{R}_{q_i}M &= \mathcal{R}(\pi, \mathbf{v}_i)M \\ &= (\mathbf{I}_3 + \sin(\mathbf{v}_i)S(\mathbf{v}_i) + (1-\cos(\pi))S(\mathbf{v}_i)^2)\sum_{j=1}^{3}\lambda_j\mathbf{v}_j\mathbf{v}_j^\top \\ &= (\mathbf{I}_3 + 2(\mathbf{v}_i\mathbf{v}_i^\top - \mathbf{I}_3))\sum_{j=1}^{3}\lambda_j\mathbf{v}_j\mathbf{v}_j^\top \\ &= 2\sum_{j=1}^{3}\lambda_j\mathbf{v}_i\mathbf{v}_i^\top\mathbf{v}_j\mathbf{v}_j^\top - \sum_{j=1}^{3}\lambda_j\mathbf{v}_j\mathbf{v}_j^\top. \end{aligned} \tag{44}$$

Since the matrix M is symmetric, then $\{\mathbf{v}_i\}_{i\in\{1,2,3\}}$ constitutes an orthonormal basis in $\mathbb{R}^3$ and, consequently, $\mathbf{v}_j^\top\mathbf{v}_i = 0$ for all $i \neq j$. Replacing this relation and $\mathbf{v}_i^\top\mathbf{v}_i = 1$ into (44) yields

$$e^{kP_M(\mathcal{R}_{q_i})S(\mathbf{u})}\mathcal{R}_{q_i}M = 2\lambda_i\mathbf{v}_i\mathbf{v}_i^\top - \sum_{j=1}^{3}\lambda_j\mathbf{v}_j\mathbf{v}_j^\top. \tag{45}$$

Using (4) we have that

$$e^{-2kP_M(\mathcal{R})S(\mathbf{u})} = \mathbf{I}_3 - \sin(2kP_M(\mathcal{R}))S(\mathbf{u}) + (1-\cos(2kP_M(\mathcal{R}))S(\mathbf{u})^2,$$

Prepared using rncauth.cls
DOI: 10.1002/rnc

and replacing this relation, (43) and (45) into (42) yields

$$\begin{aligned}\mu(\mathscr{V}) = \max\big\{0,\\ \min_{\substack{q\in Q\\ i\in\{1,2,3\}}} \; & (1-\cos(2kP_M(\mathcal{R}_{q_i})))\,\mathrm{trace}((\mathbf{u}\mathbf{u}^\top - \mathbf{I})(2\lambda_i\mathbf{v}_i\mathbf{v}_i^\top - \sum_{j=1}^{3}\lambda_j\mathbf{v}_j\mathbf{v}_j^\top))\\ & - \sin(2kP_M(\mathcal{R}_{q_i}))\,\mathrm{trace}(S(\mathbf{u})(2\lambda_i\mathbf{v}_i\mathbf{v}_i^\top - \sum_{j=1}^{3}\lambda_j\mathbf{v}_j\mathbf{v}_j^\top))\big\}.\end{aligned} \tag{46}$$

Notice that, using the property $\mathrm{trace}(AB) = \mathrm{trace}(BA)$, $\mathrm{trace}(S(\mathbf{u})\mathbf{v}\mathbf{v}^\top) = \mathbf{v}^\top S(\mathbf{u})\mathbf{v} = 0$ for all $\mathbf{v}\in\mathbb{R}^3$, because the quadratic form of a skew symmetric matrix is always 0, thus we may drop the last term in (46). With some additional computations we may rewrite (46) as

$$\begin{aligned}\mu(\mathscr{V}) = \max\big\{0,\\ \min_{\substack{q\in Q\\ i\in\{1,2,3\}}} \; & (1-\cos(2kP_M(\mathcal{R}_{q_i})))\,\mathrm{trace}(\sum_{j=1}^{3}\lambda_j(1-(\mathbf{u}^\top\mathbf{v}_j)^2) - 2\lambda_i(1-(\mathbf{u}^\top\mathbf{v}_i)))\big\}.\end{aligned}$$

From (25) we have that $0 < k < (\sqrt{2}\|\boldsymbol{\lambda}\|_2)^{-1}$ where $\boldsymbol{\lambda} := \begin{bmatrix}\lambda_1 & \lambda_2 & \lambda_3\end{bmatrix}^\top$ and from the properties of the modified trace function of matrix M we have that $P_M(\mathcal{R}_{q_i}) < \|\boldsymbol{\lambda}\|_1$. Using the property $\|\boldsymbol{\lambda}\|_1 \leq \sqrt{3}\|\boldsymbol{\lambda}\|_2$ we conclude that

$$0 < 2kP_M(\mathcal{R}_{q_i}) < \sqrt{6},$$

which in turn implies that $1-\cos(2kP_M(\mathcal{R}_{q_i})) > 0$ for all $\mathcal{R}_{q_i}\in \mathrm{Crit}\, V_q\backslash\{\mathbf{I}_3\}$. We may conclude that the synergy gap $\mu(\mathscr{V})$ is greater than 0 if and only if (26) is verified. □

DOI: 10.1002/rnc